The Photon Strength Function & Its Impact on Nucleosynthesis

S. Goriely
IAA-ULB, Belgium

- Introduction to Nucleosynthesis of the elements heavier than Fe
- Photon strength functions
  - Existing PSF models for applications
  - Experimental constraints
  - The new de-excitation D1M+QRPA PSF
- PSF uncertainty propagation & impact on Nucleosynthesis

In collaboration with S. Hilaire and S. Péru (CEA/DAM)

The various nucleosynthesis processes for elements heavier than Fe

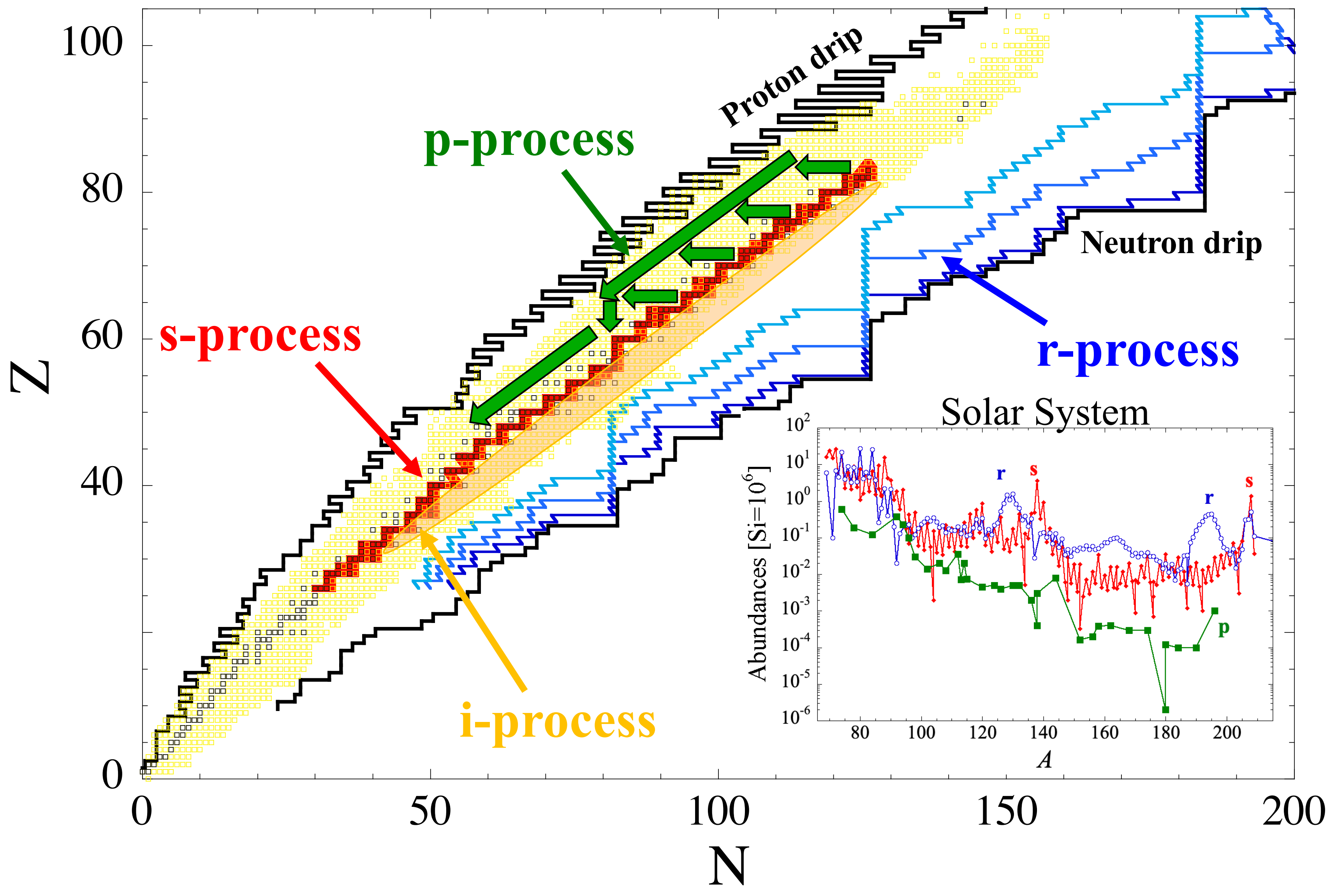

The slow neutron-capture process (or s-process)

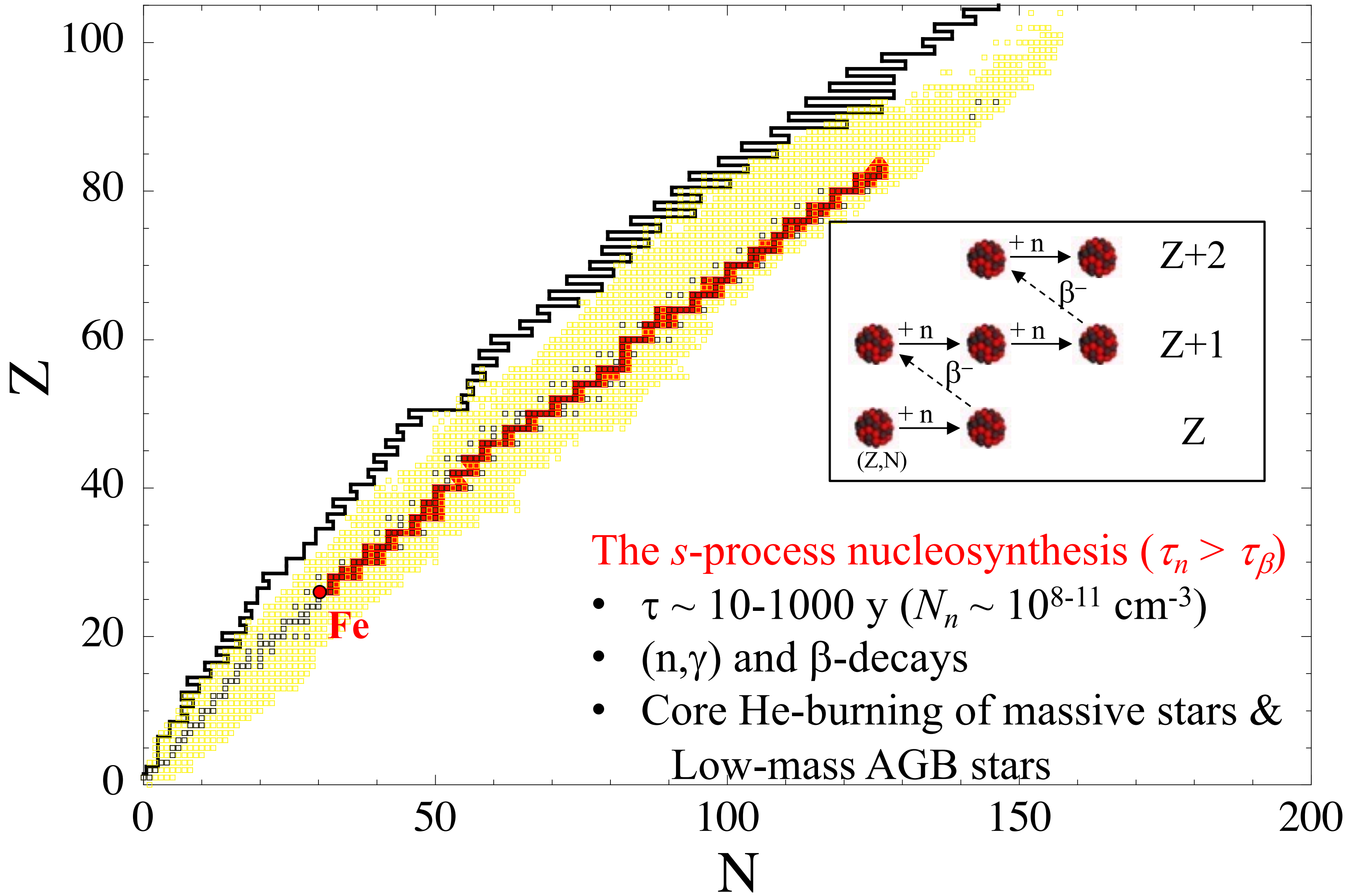

- The s-process is responsible for about half of the elements heavier than iron in the Universe
- Most of the nuclear inputs are based on experimental data, including measured (n,γ) rates

The rapid neutron-capture process (or r-process)

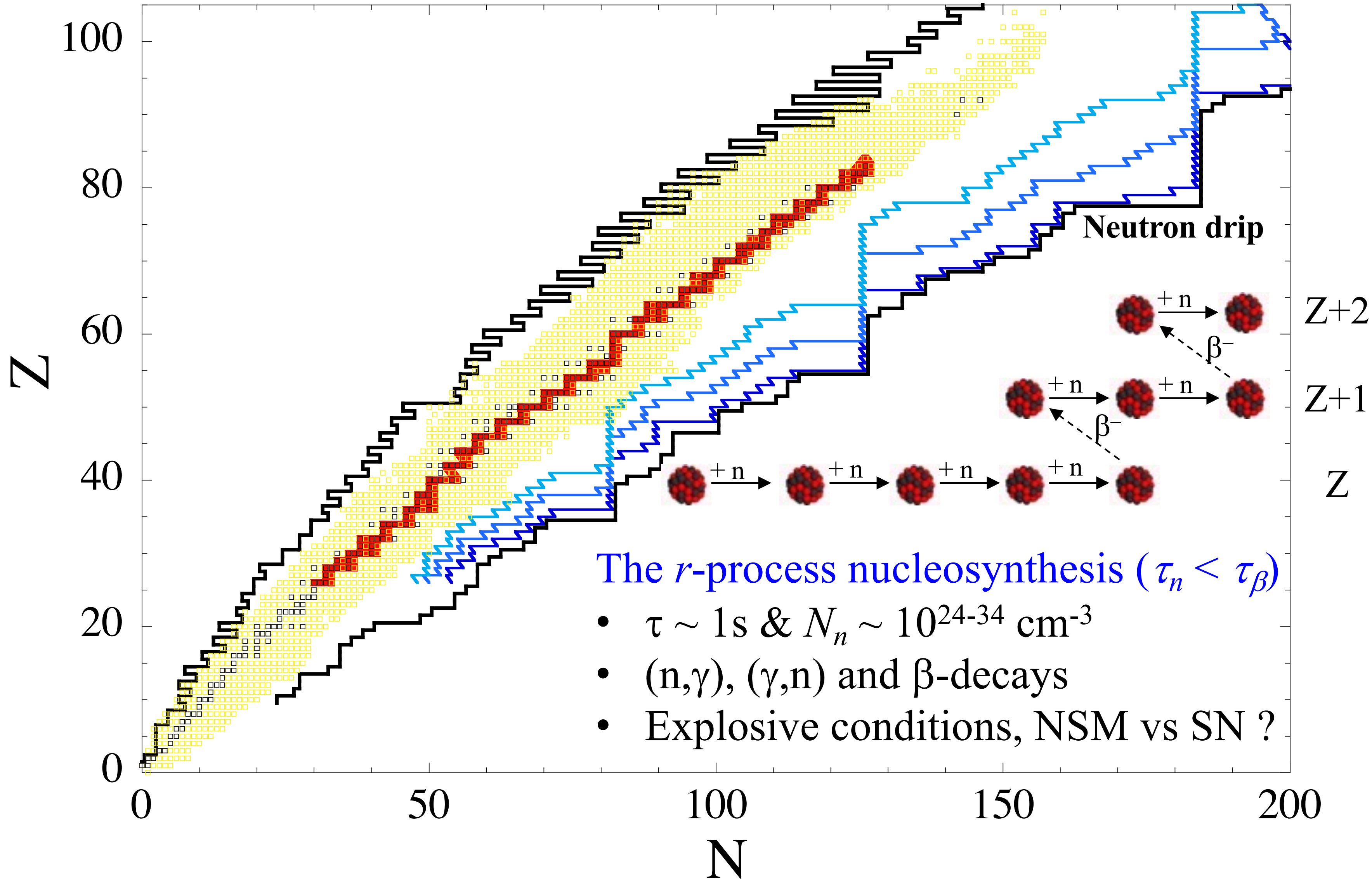

- The r-process is responsible for about half of the elements heavier than iron in the Universe

The r-process nucleosynthesis responsible for half the elements heavier than iron in the Universe

one of the still unsolved puzzles in nuclear astrophysics

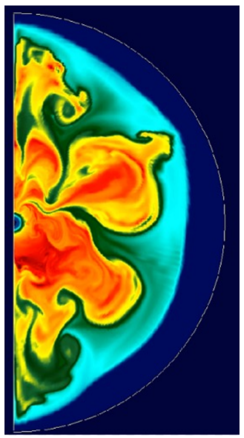

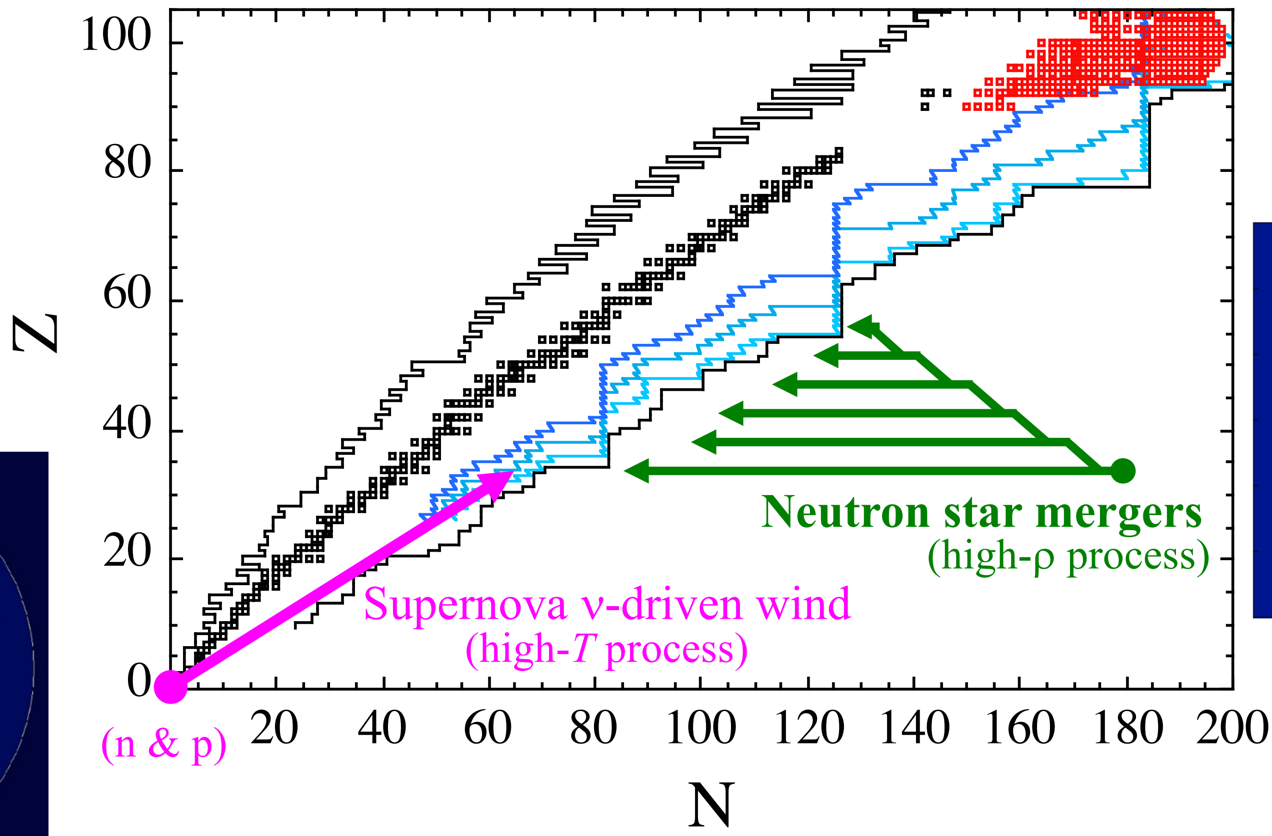

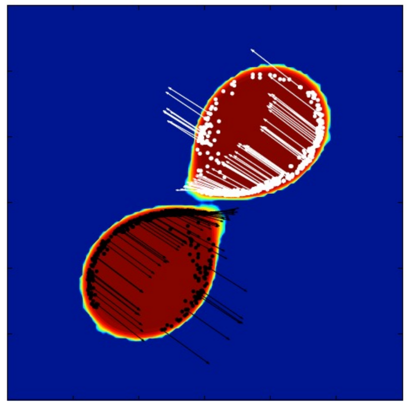

Nuclear physics input to the r-process nucleosynthesis

(n,γ) – (γ,n) – β competition & Fission

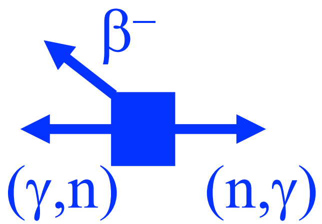

- β-decay **rates**
- (n,γ) and (γ,n) **rates**
- Fission (nif, sf, βdf) **rates**
- Fission Fragments Distributions

Simulations rely almost entirely on theory

~ 5000 nuclei involved – almost no exp. data – still many open questions

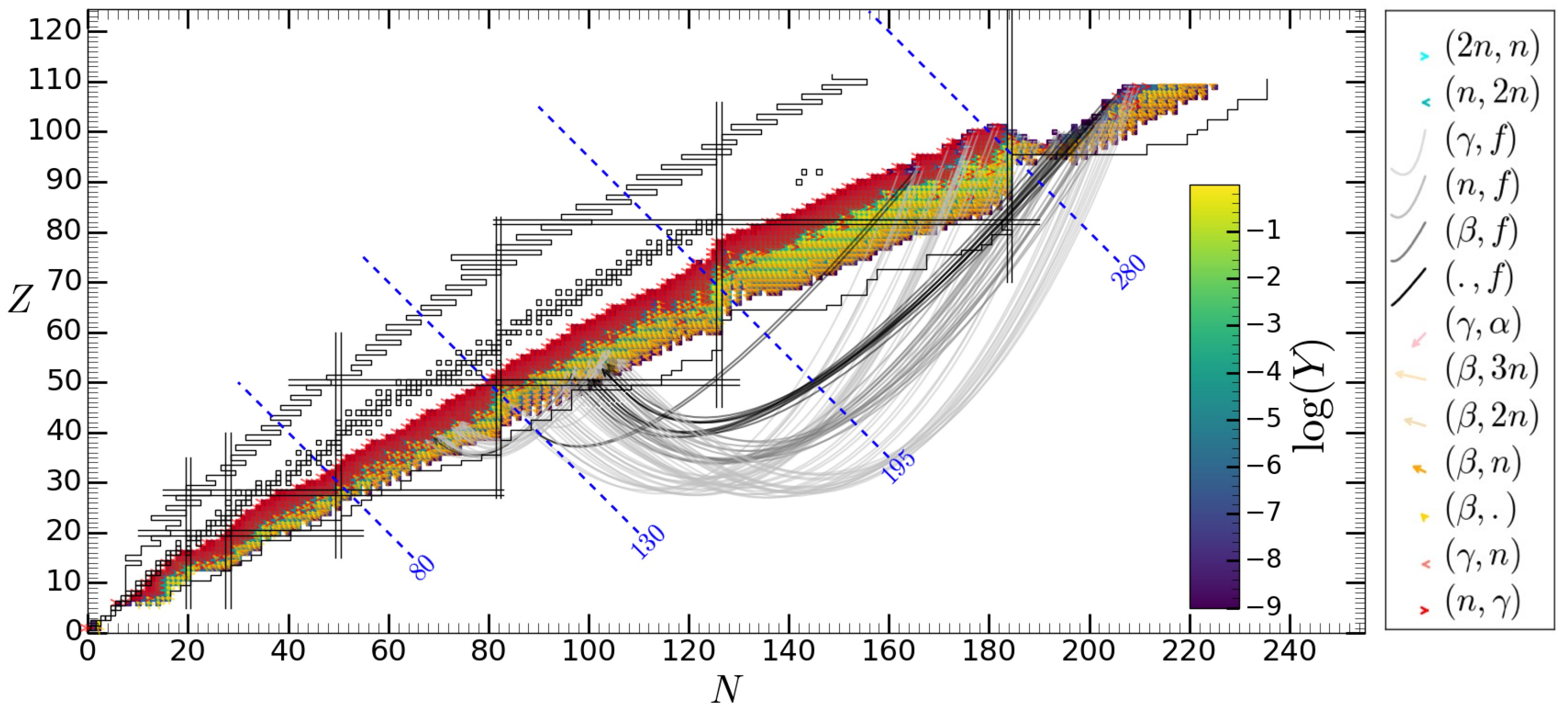

What about an intermediate neutron-capture process ?

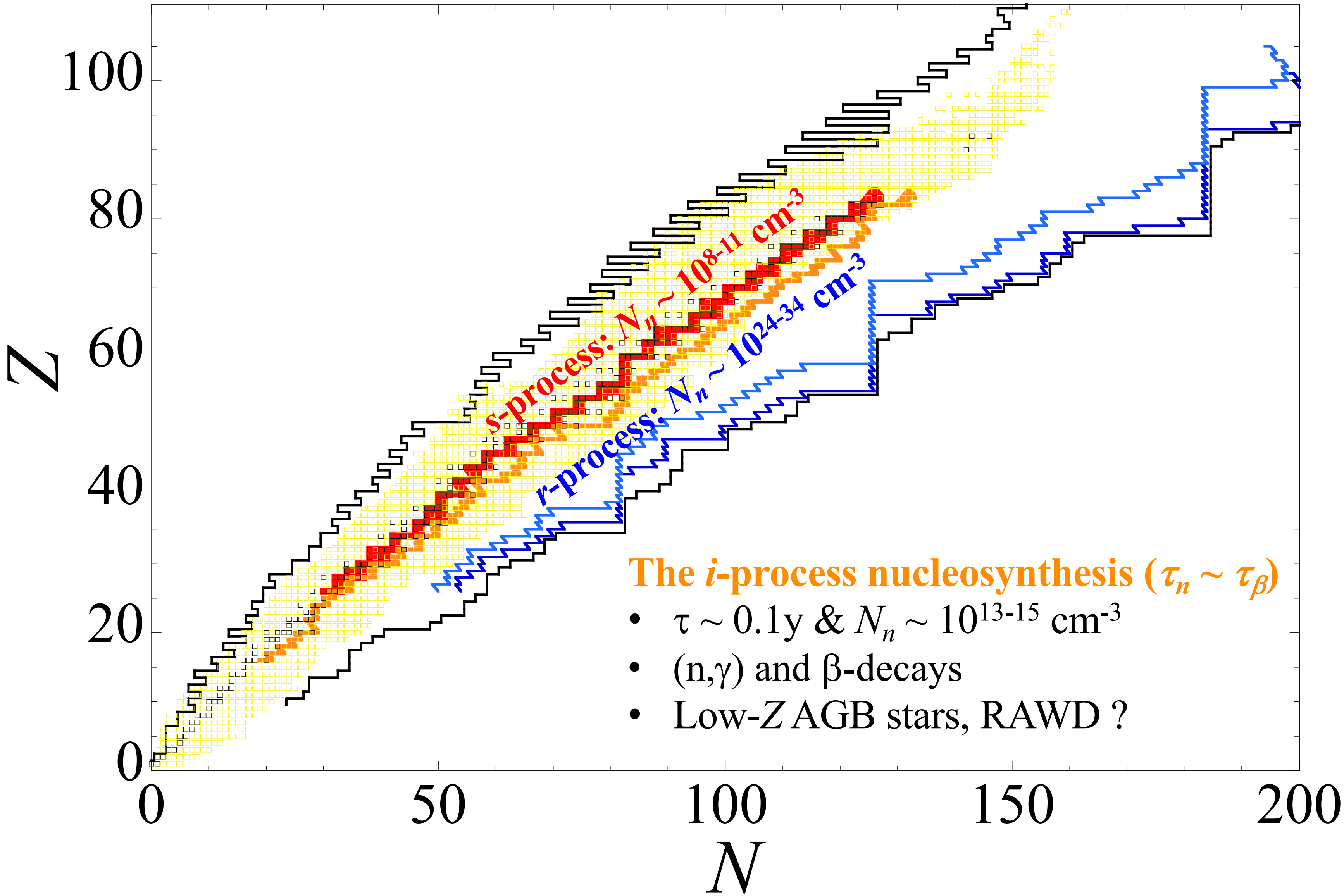

- The *i*-process may not contribute to the SoS but is required to explain CEMP-rs stars
- Important part of the nuclear inputs are based on predictions, in particular (n,γ) rates

The p-process nucleosynthesis

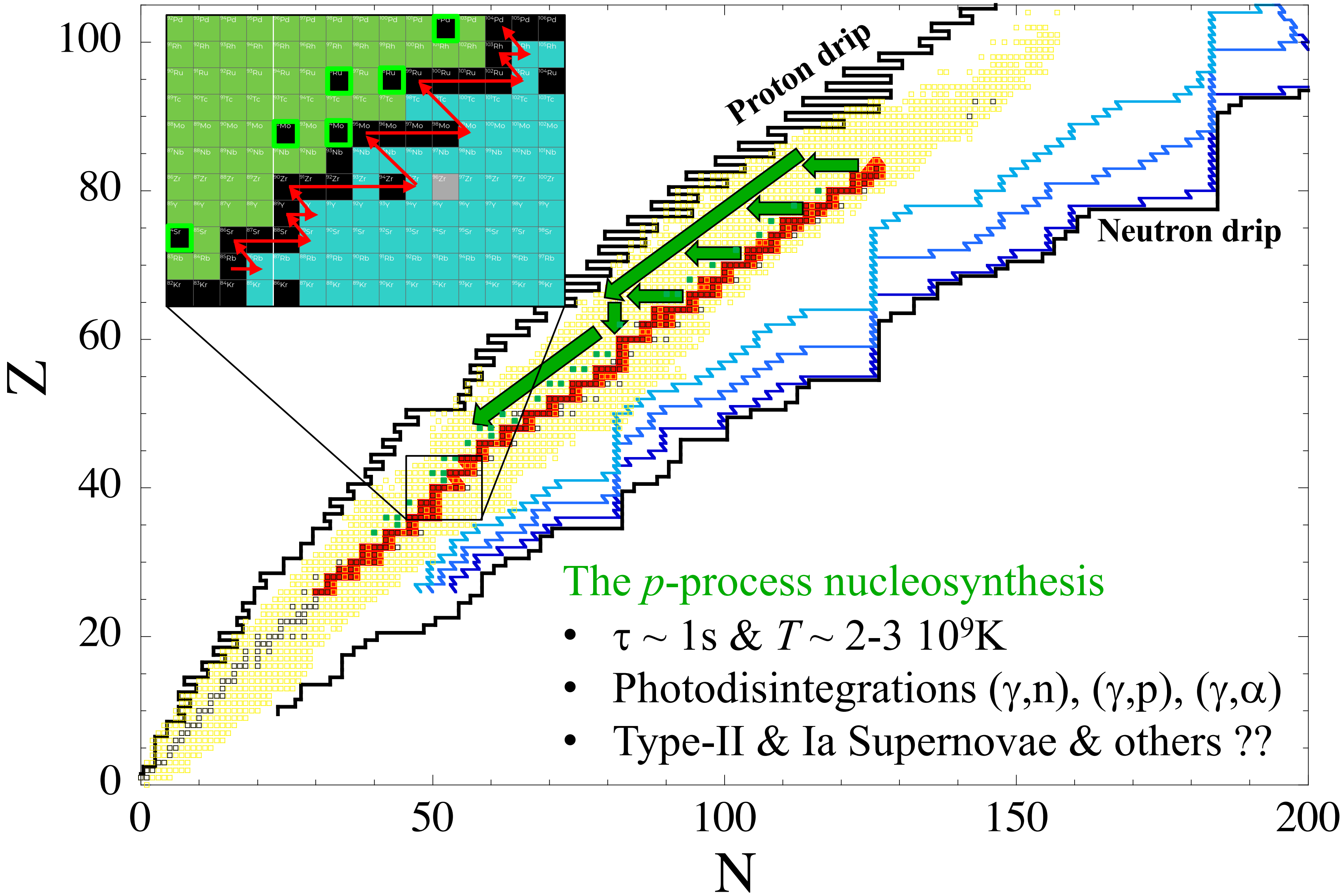

The *p*-process nucleosynthesis

- $\tau \sim 1$s & $T \sim$ 2-3 10^9K
- Photodisintegrations (γ,n), (γ,p), (γ,α)
- Type-II & Ia Supernovae & others ??

Many different nuclear needs for the various nucleosynthesis processes

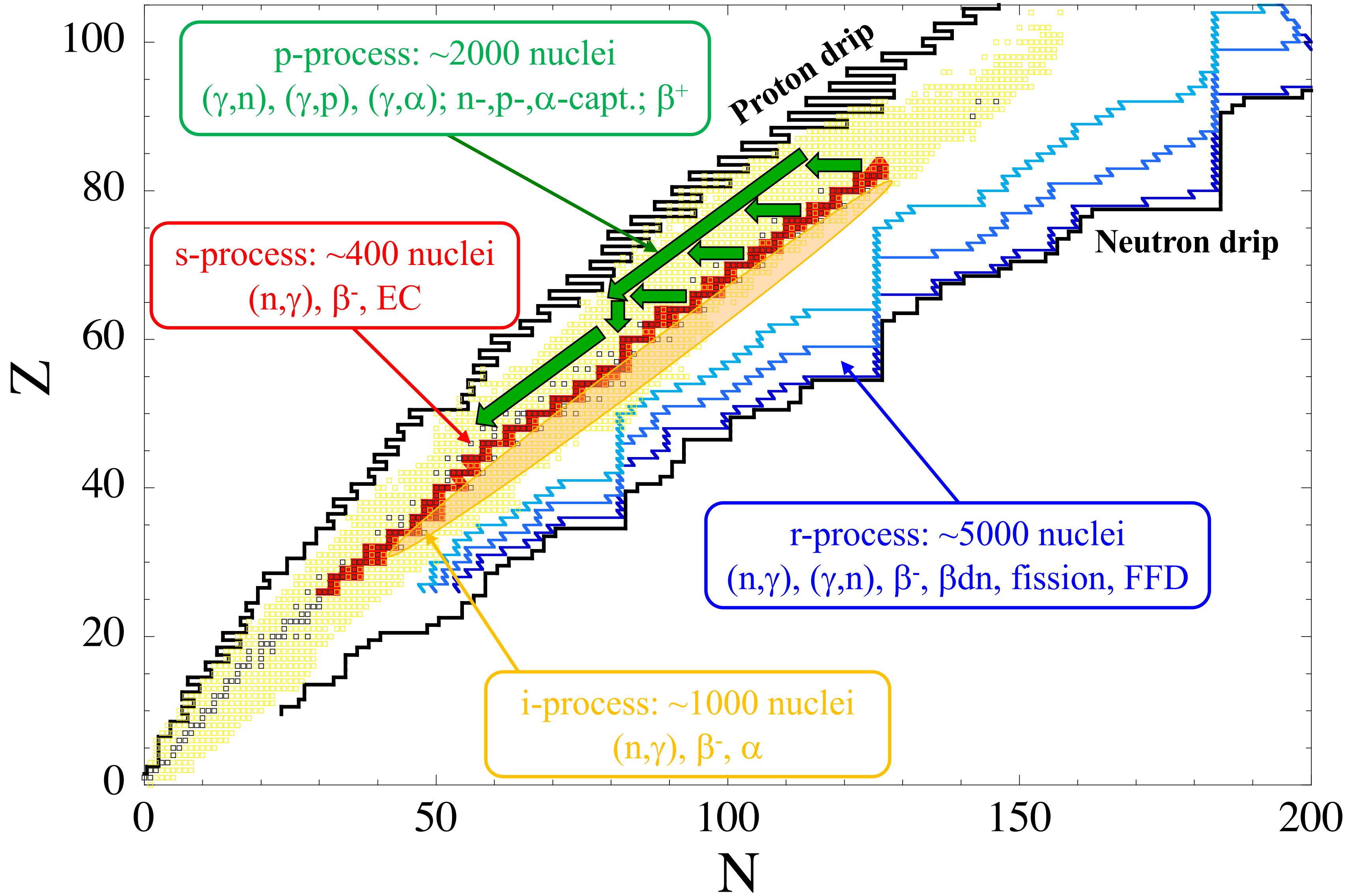

For heavy nuclei, essentially - *Radiative* neutron capture reactions (E_n~10-100keV)

- *Photon*-induced reactions (T~2-3 10^9K)

Hauser-Feshbach model for radiative neutron capture reactions

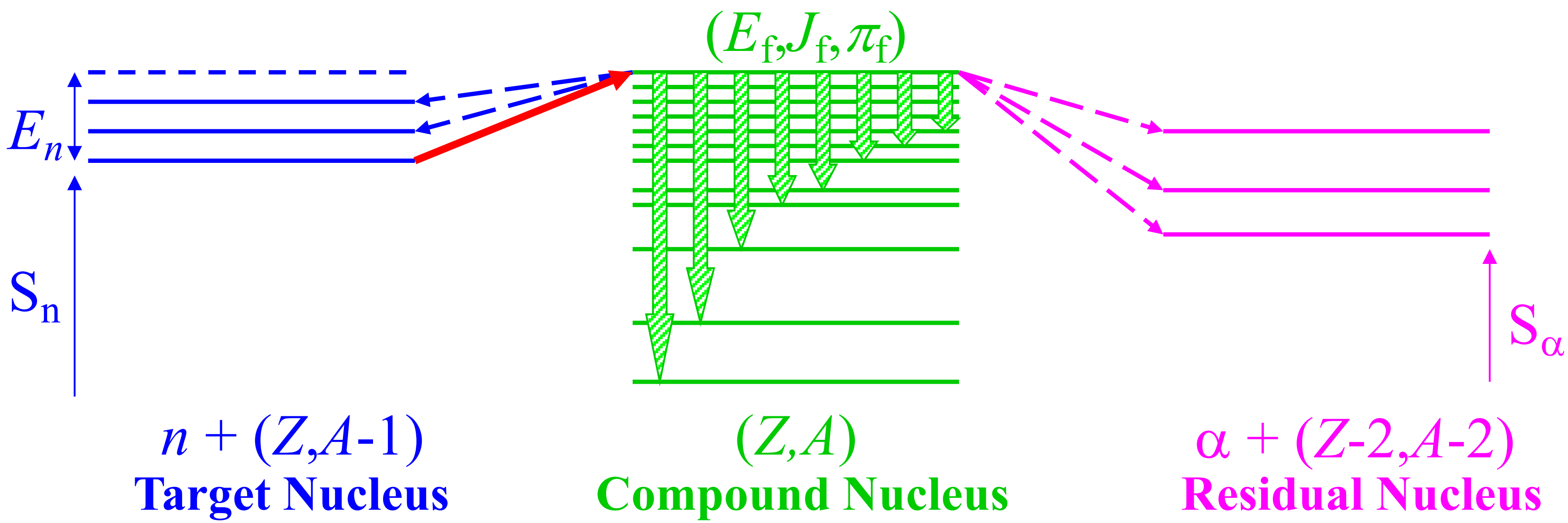

$$\sigma_{(n,\gamma)} \propto \sum_{J,\pi} \frac{T_n(J^\pi)T_\gamma(J^\pi)}{T_n(J^\pi)+T_\gamma(J^\pi)} \approx \sum_{J,\pi} T_\gamma(J^\pi) \quad \text{since } T_n(J^\pi) >> T_\gamma(J^\pi) \text{ for } E_n \sim \text{keV}$$

$$T_\gamma = \sum_{J^\pi XL} \int_0^{S_n+E_n} 2\pi\varepsilon_\gamma^{2L+1} f_{XL}(\varepsilon_\gamma)\rho(S_n+E_n-\varepsilon_\gamma, J, \pi)\, d\varepsilon_\gamma$$

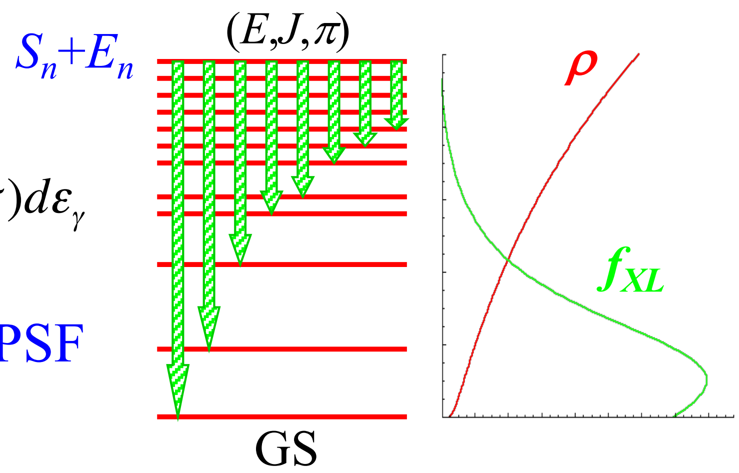

Nuclear astrophysics apps require NLDs & PSF for ~ 8000 nuclei

Detailed balance and reverse reactions in stellar conditions

Reverse reactions can be estimated with the use of the reciprocity theorem. In particular, the stellar photo-dissociation rates (in s^{-1}) are classically derived from the reverse radiative capture rates by

$$\boxed{\lambda^{*}_{(\gamma,j)}(T) = \frac{(2J_I^0+1)(2J_j+1)}{(2J_L^0+1)}\,\frac{G_I(T)}{G_L(T)}\left(\frac{mkT}{2\pi\hbar^2}\right)^{3/2}\langle\sigma v\rangle^{*}_{(j,\gamma)}\ \mathrm{e}^{-Q_{j\gamma}/kT}}$$

where $Q_{j\gamma}$ is the Q-value of the $I^0(j,\gamma)L^0$ capture reaction and $G_I(T) = \sum_{\mu}\frac{2J_I^{\mu}+1}{2J_I^0+1}\exp\left(-\frac{\varepsilon_I^{\mu}}{kT}\right)$

Note that, in stellar conditions, the reaction rates for targets in thermal equilibrium obey reciprocity since the forward and reverse channels are symmetrical, in contrast to the situation which would be encountered for targets in their ground states only.

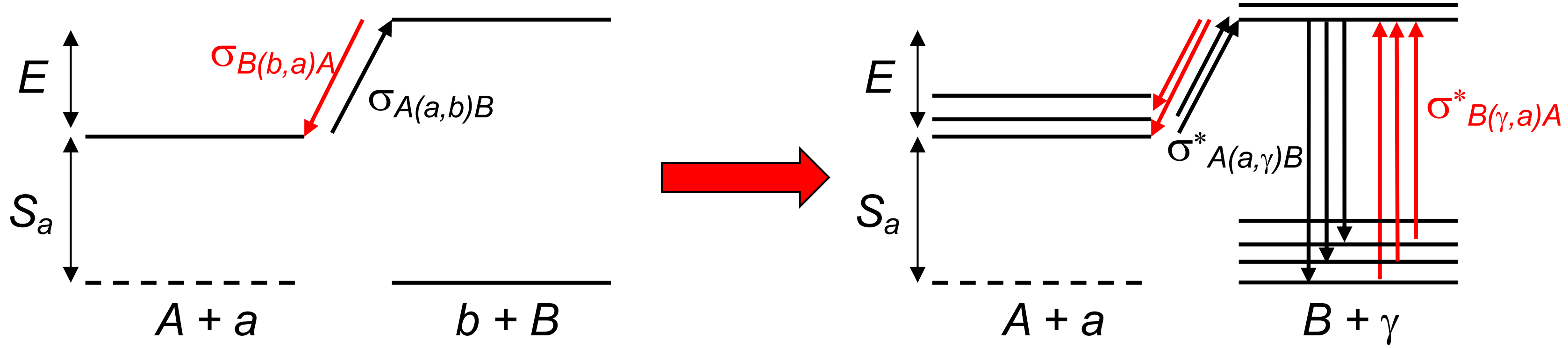

The Lorentzian model of the dipole strength function

- *E1 strength function*
  - Standard Lorentzian (E_0, Γ_0, σ_0)
  - Lorentzian with E-dependent width
  - Generalized Lorentzian with T- and E-dep. width

    → at the basis of GLO, EGLO, MLO, SMLO, Hybrid, … models

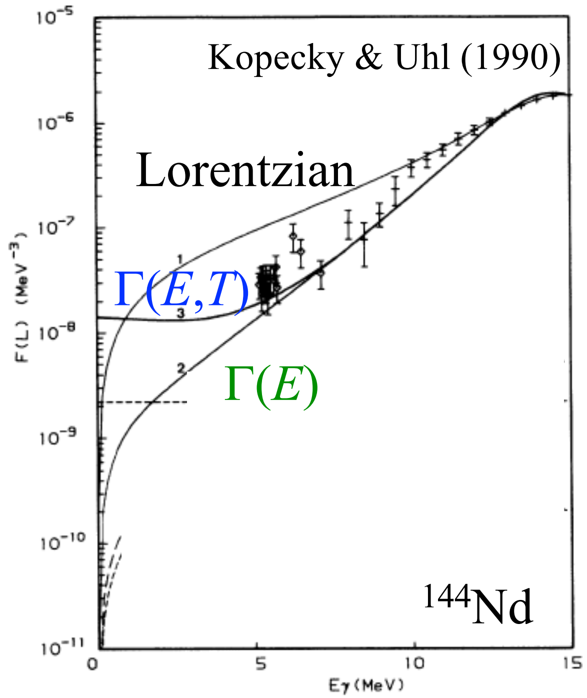

- *M1 strength function*

SLO (Kopecky & Uhl 1990) - SMLO (SG & Plujko 2019)

$$\overrightarrow{f_{M1}}(\varepsilon_\gamma) = \frac{1}{3\pi^2\hbar^2c^2}\sigma_{sc}\frac{\varepsilon_\gamma\,\Gamma_{sc}^2}{(\varepsilon_\gamma^2 - E_{sc}^2)^2 + \varepsilon_\gamma^2\Gamma_{sc}^2}$$ Scissors mode for deformed nuclei

$$+\frac{1}{3\pi^2\hbar^2c^2}\sigma_{sf}\frac{\varepsilon_\gamma\,\Gamma_{sf}^2}{(\varepsilon_\gamma^2 - E_{sf}^2)^2 + \varepsilon_\gamma^2\Gamma_{sf}^2}$$ Spin-Flip mode

Two variants considered here for both E1 & M1
- **GLO** (Kopecky & Uhl 1990) - Still extensively used
- **SMLO** (SG & Plujko 2019) - Updated version

The Mean Field + QRPA model of the dipole strength function

Large-scale $E1/M1$ Mean-Field + QRPA calculations

Skyrme-HFB + QRPA	Gogny-HFB + QRPA	RMF +QRPA

QRPA calculations can *accurately* reproduce experimental data, provided empirical corrections are made, *i.e.*

- beyond QRPA excitations and phonon couplings → Empirical *energy shift*
- Empirical damping of collective motions → Empirical *broadening*
- Spherical calculations → Empirical *deformation effects*
- Approximation / Interpolation for *odd systems*

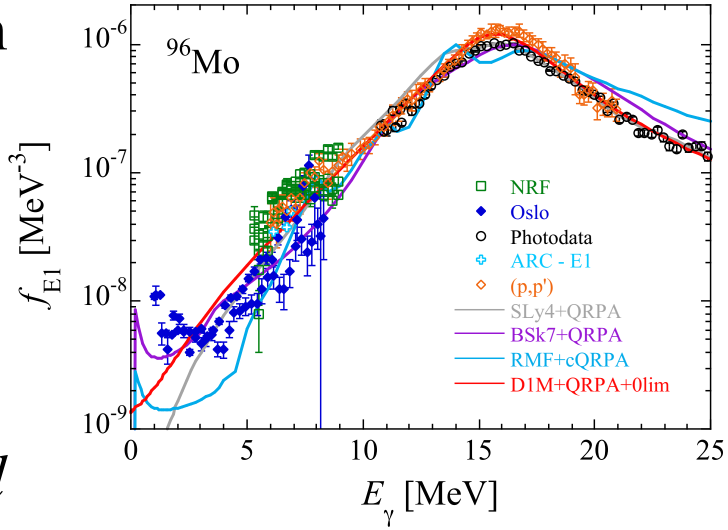

of particular relevance for a ”reliable” prediction of experimentally unknown nuclei, hence for astrophysical applications

The Mean Field + QRPA model of the dipole strength function

Large-scale $E1/M1$ Mean-Field + QRPA calculations

Skyrme-HFB + QRPA	Gogny-HFB + QRPA	RMF +QRPA

QRPA calculations can *accurately* reproduce experimental data, provided empirical corrections are made, *i.e.*

- beyond QRPA excitations and phonon couplings
  → Empirical *energy shift*
- Empirical damping of collective motions
  → Empirical *broadening*
- Spherical calculations → Empirical *deformation effects*
- Approximation / Interpolation for *odd systems*

Large-scale Gogny-HFB + QRPA calculations:
Consistent axially deformed calculation of E1 & M1 PSF
for e-e nuclei with $8 \leq Z \leq 110$
on the basis of the D1M Gogny force: **D1M+QRPA**

Possible additional low-energy contribution to the **dipole de-excitation strength function**

Violation of the Brink hypothesis (e.g. Isaak et al., 2019)

$$\overleftarrow{f}_{E1}(\varepsilon_\gamma) \neq \overrightarrow{f}_{E1}(\varepsilon_\gamma)$$

$$\overleftarrow{f}_{E1} = \overleftarrow{f}_{E1}(\varepsilon_\gamma, T_f)$$

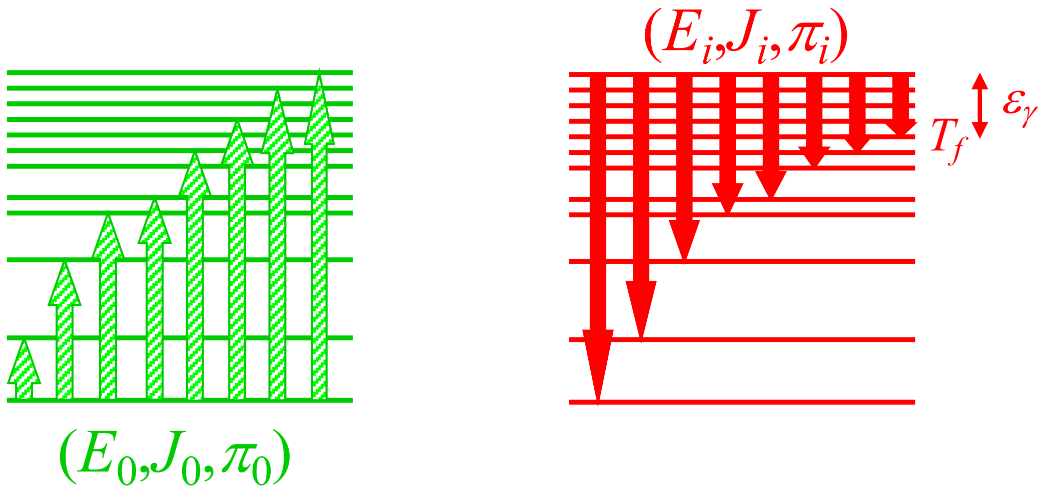

SM-inspired low-energy correction of the de-excitation strength

$$f_{E1} = f_{E1}^{QRPA} + f_{E1}(\varepsilon_\gamma \to 0)$$ Non-zero limit of the *E1* strength at $\varepsilon_\gamma \to 0$

$$f_{M1} = f_{M1}^{QRPA} + f_{M1}(\varepsilon_\gamma \to 0)$$ Upbend of the *M1* strength at $\varepsilon_\gamma \to 0$

D1M+QRPA+0lim model

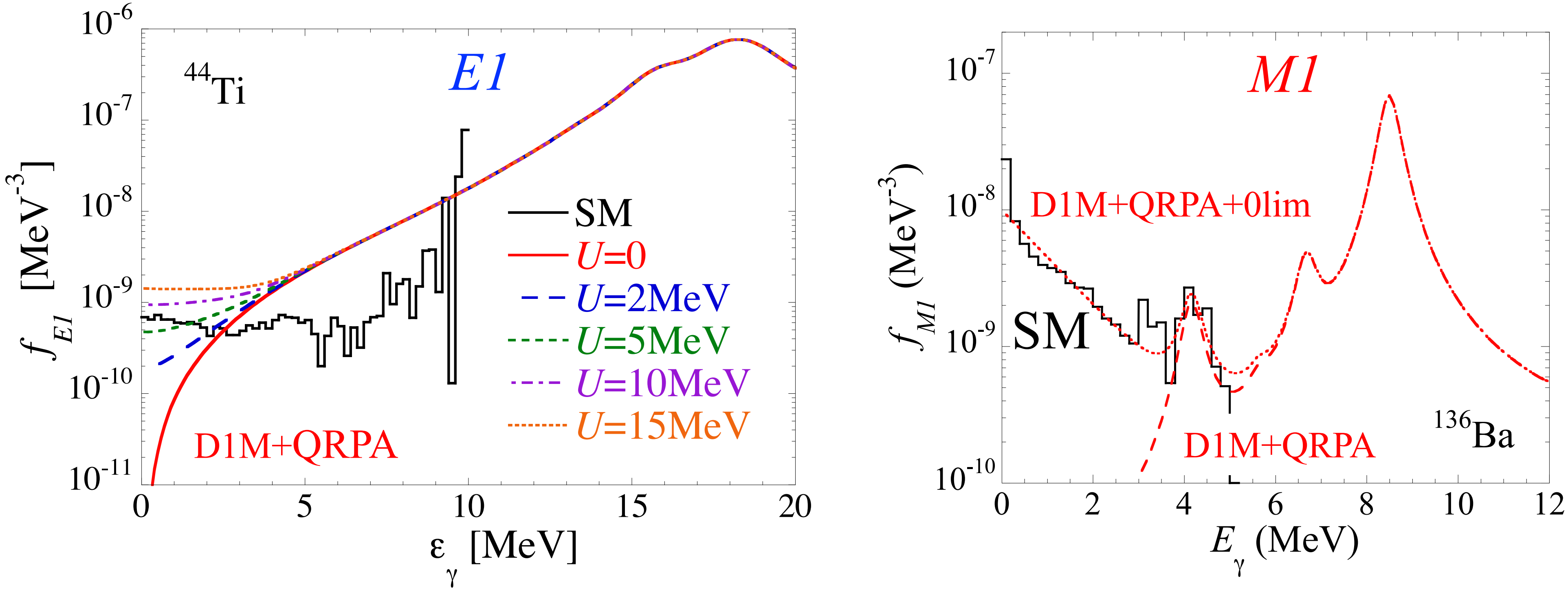

Schwengner et al. (2013, 2017), Brown et al. (2014), Sieja (2017, 2018), Karampagia et al. (2017), Midtbø et al. (2018)

SM-inspired low-energy correction of the de-excitation strength

$$f_{E1} = f_{E1}^{QRPA} + f_{E1}(\varepsilon_\gamma \to 0)$$ Non-zero limit of the *E1* strength at $\varepsilon_\gamma \to 0$

$$f_{M1} = f_{M1}^{QRPA} + f_{M1}(\varepsilon_\gamma \to 0)$$ Upbend of the *M1* strength at $\varepsilon_\gamma \to 0$

D1M+QRPA+0lim model

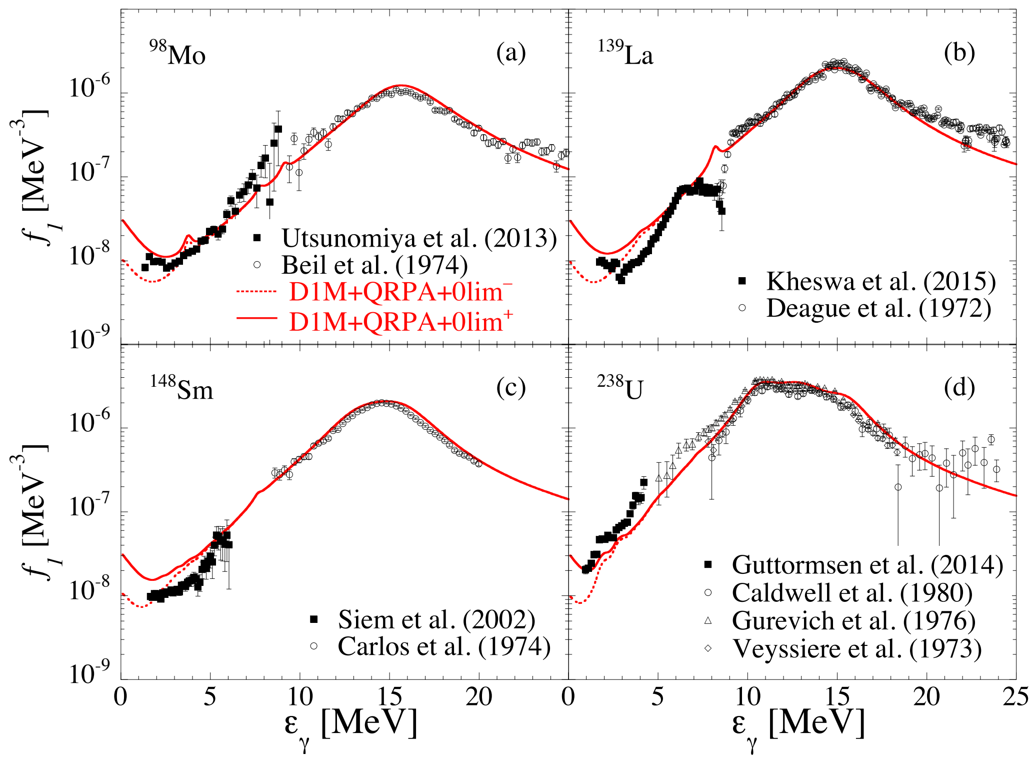

Oslo data

Major questions related to the dipole PSF for astrophysics applications (~8000 nuclei)

E1 strength

→ Centroid energy and width of the GDR for experimentally unknown nuclei ?

→ Presence of a *E1* pygmy resonance or more generally low-*E* tail of the GDR ?

→ Non-zero limit of the *E1* strength (*T*-effect ?)

M1 strength

→ Properties of the *M1* Spin-flip strength ?

→ Properties of *M1* Scissors mode ?

→ Non-zero limit of the *M1* strength (upbend) ?

"Validation" of the theoretical dipole Photon Strength Function on

IAEA Reference Database developed within the 2016-2019 CRP

1. Photodata in the GDR region (10-20MeV): *E1* for ~159 nuclei
2. ARC/DRC data: $\varepsilon_\gamma \sim$ 5-8MeV; *E1* & *M1* for 88 nuclei
3. Oslo data: $\varepsilon_\gamma < S_n$; *E1*+*M1* for 72 nuclei
4. NRF data: $\varepsilon_\gamma < S_n$; *E1*+*M1* for 23 nuclei
5. $\Sigma B(M1)$ scattering data: $\varepsilon_\gamma \sim$ 2-4MeV for ~47 nuclei
6. (p,γ) data: *E1*+*M1* at $\varepsilon_\gamma \sim$ 5-10MeV for 22 nuclei ($A = 46 - 90$)
7. (p,p') data for ^{96}Mo, ^{120}Sn, ^{208}Pb: *E1* & *M1* at $\varepsilon_\gamma \sim$ 5-20MeV
8. MSC & MD spectra: *E1*+*M1* for ~15 nuclei with ~4 J^π/nuc (NLD)
9. Neutron capture spectra: *E1*+*M1* for 5 nuclei & diff J^π (NLD)
10. Average radiative width $<\Gamma_\gamma>$: $0 \leq \varepsilon_\gamma \leq S_n$ *E1*+*M1* for ~230 nuc (NLD)
11. 30keV MACS $0 \leq \varepsilon_\gamma \leq S_n$ *E1*+*M1* for ~240 nuc (NLD)

PSF database (*https://www-nds.iaea.org/PSFdatabase*) regularly updated

IAEA Reference Database for Photon Strength Functions

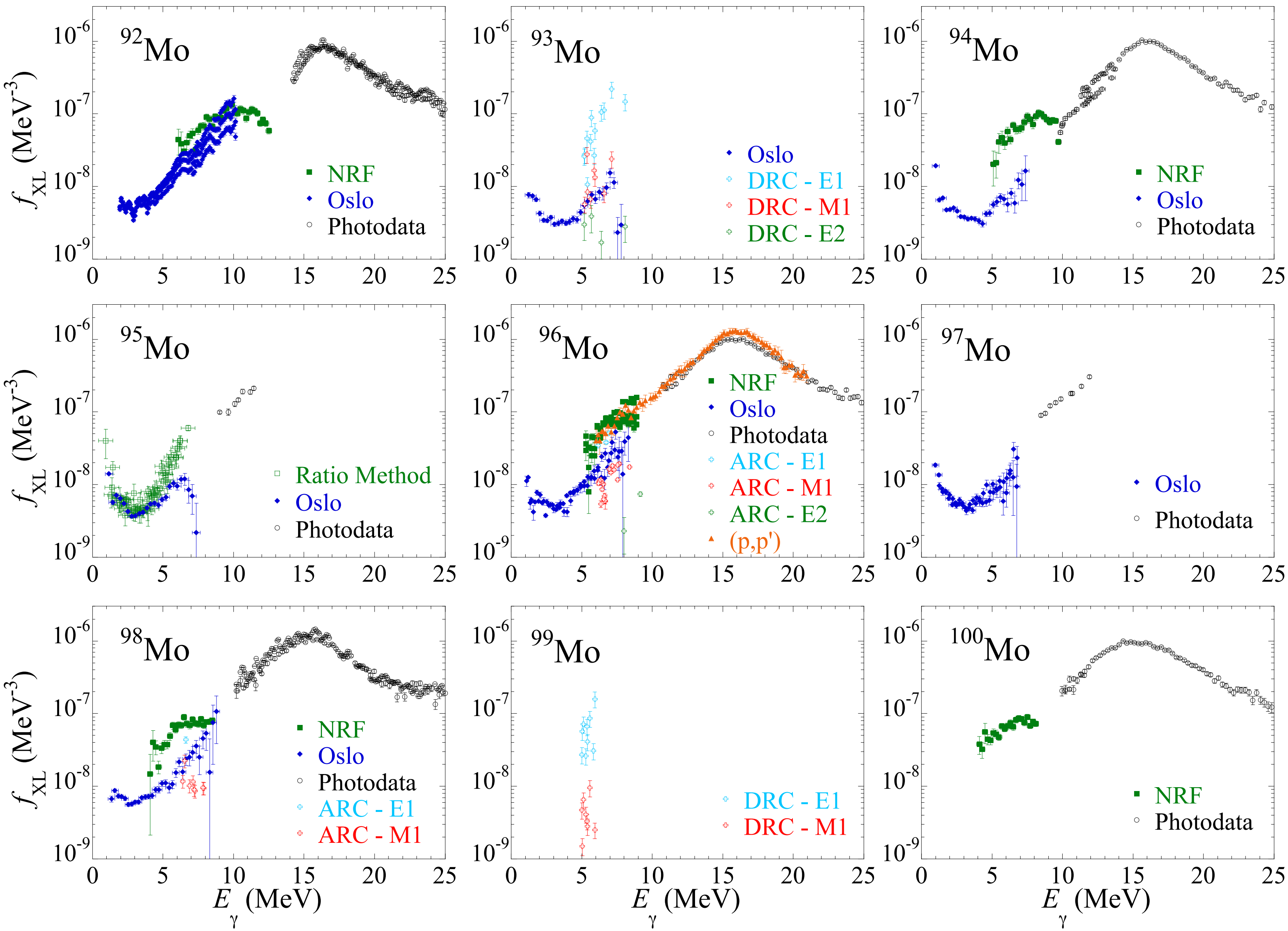

Requires further "evaluation" and detailed uncertainty analysis

Comparison between Oslo and NRF data

9 nuclei
measured by
both techniques

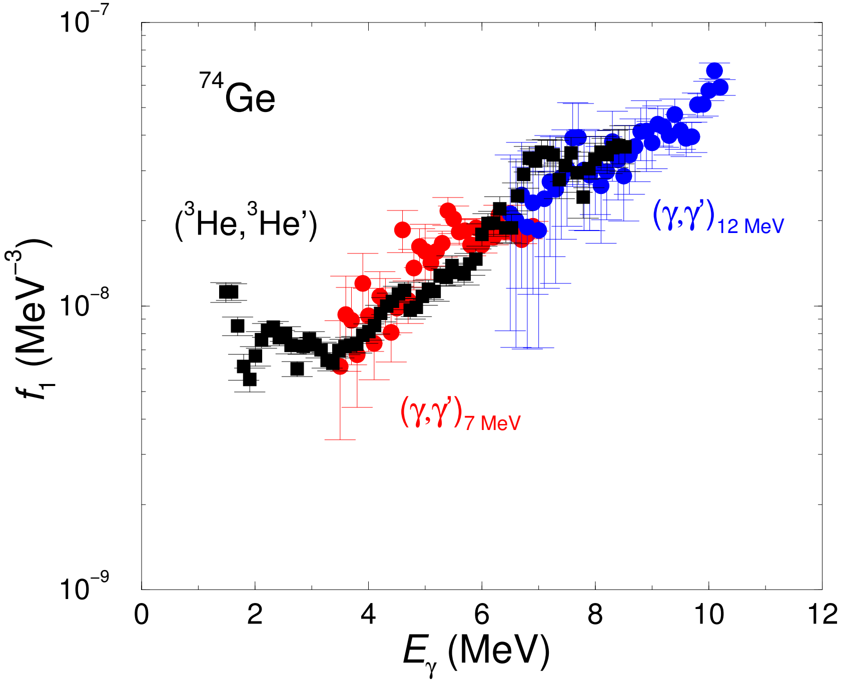

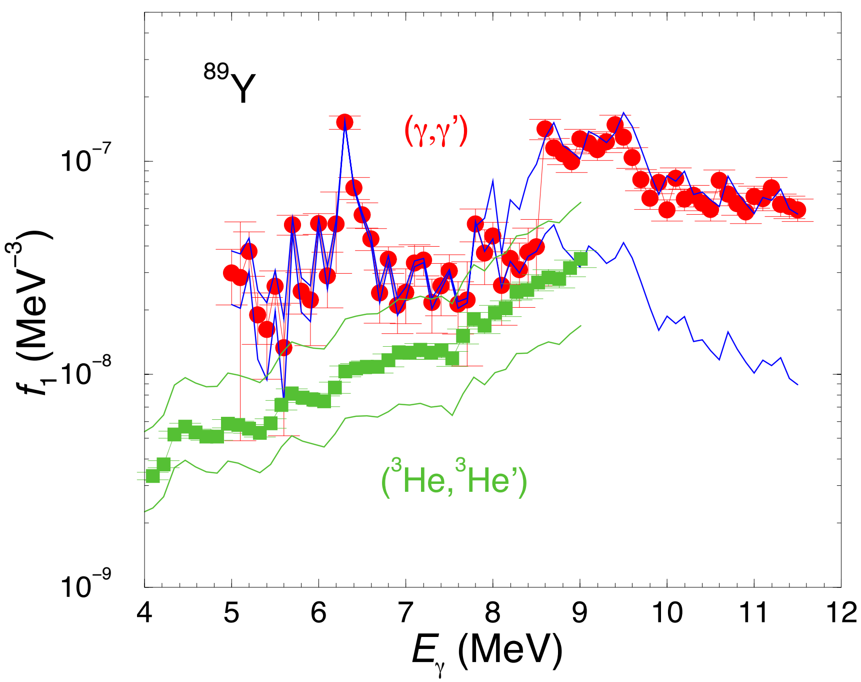

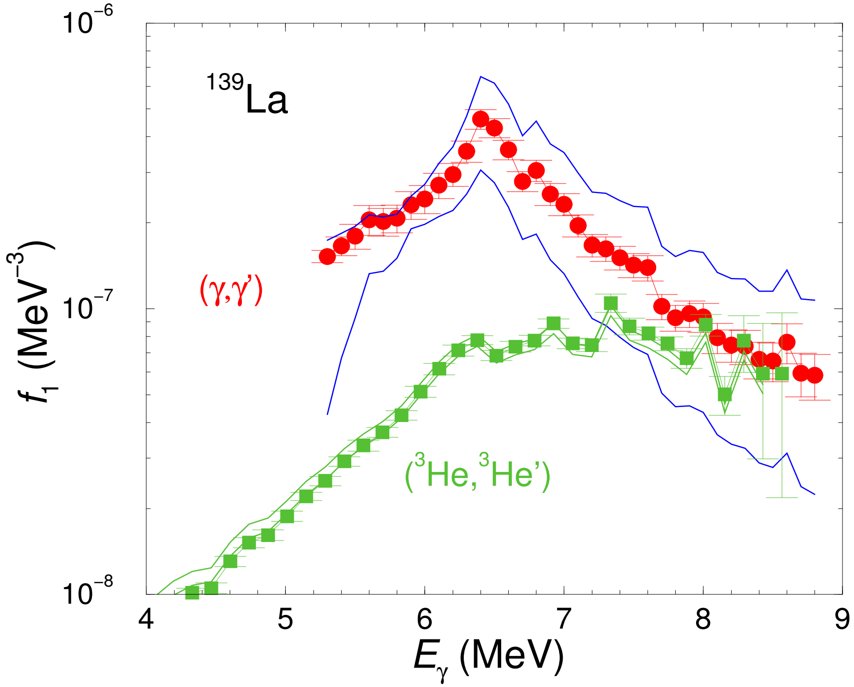

Comparison of D1M+QRPA and SMLO with Photodata

30 nuclei out of 159

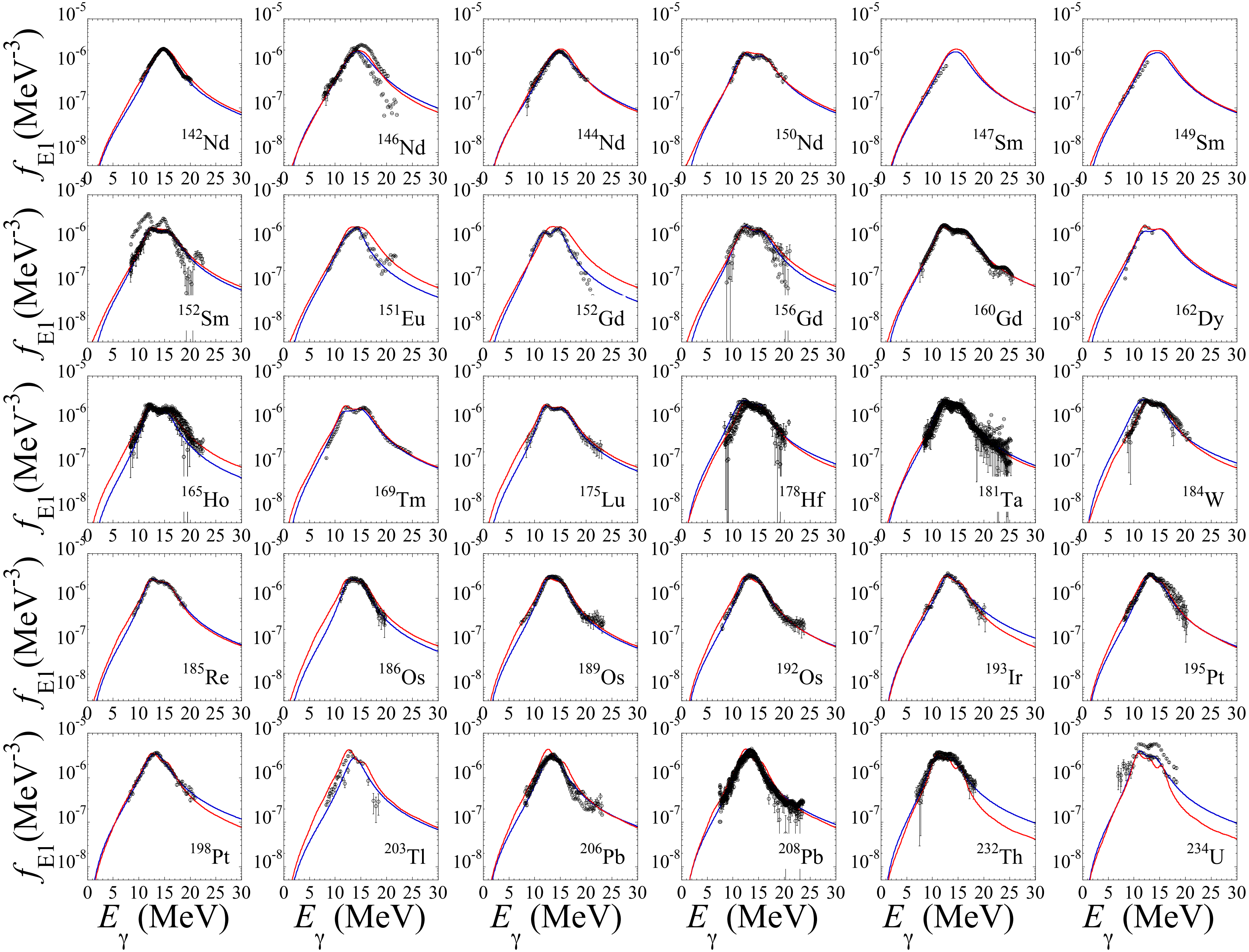

Comparison of D1M+QRPA and SMLO with NRF data

23 nuclei

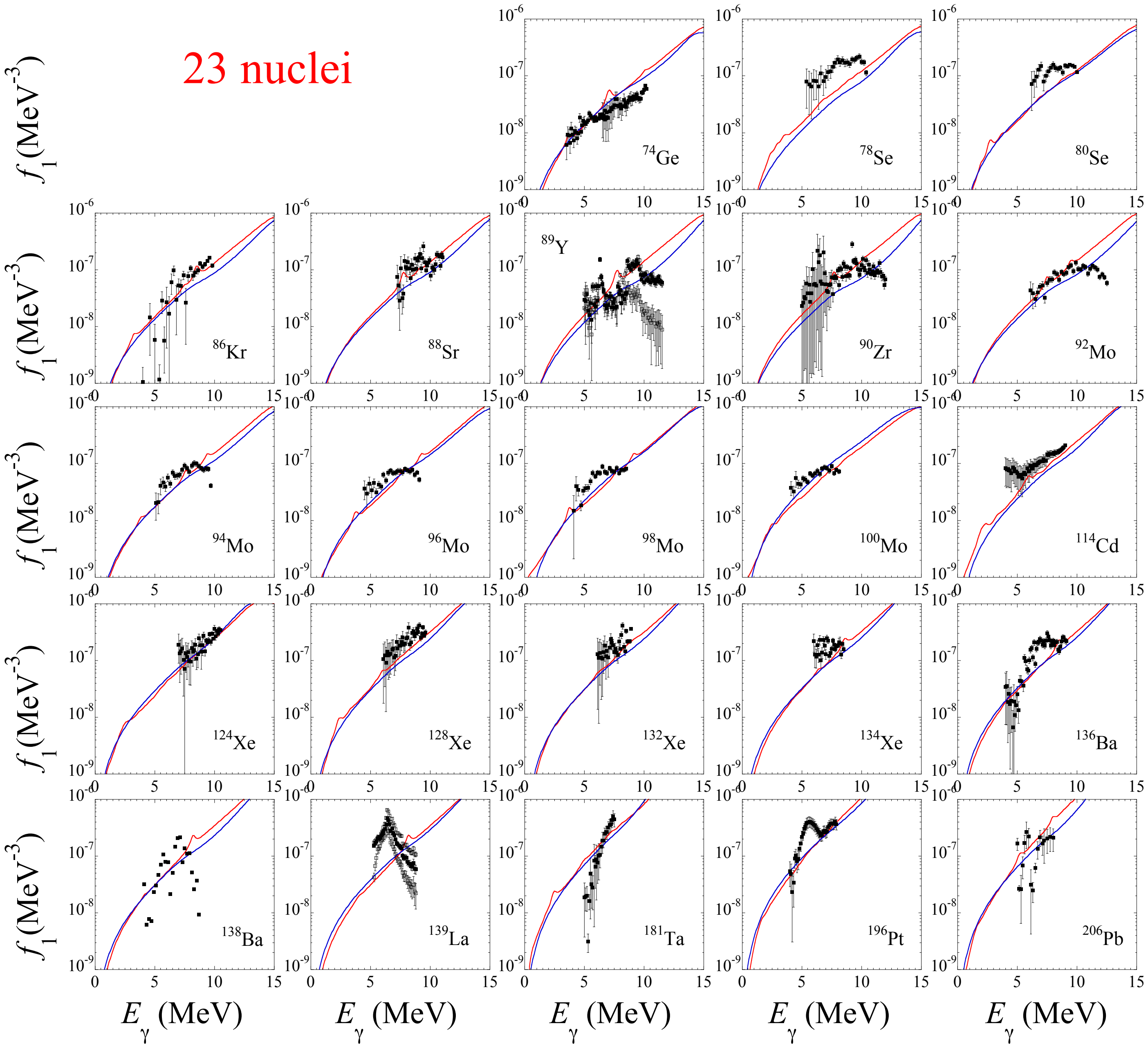

Comparison with E1 and M1 ARC data (Kopecky 2019)

25 nuclei out of 88

D1M+QRPA+0lim ——— **SMLO** - - - - - -

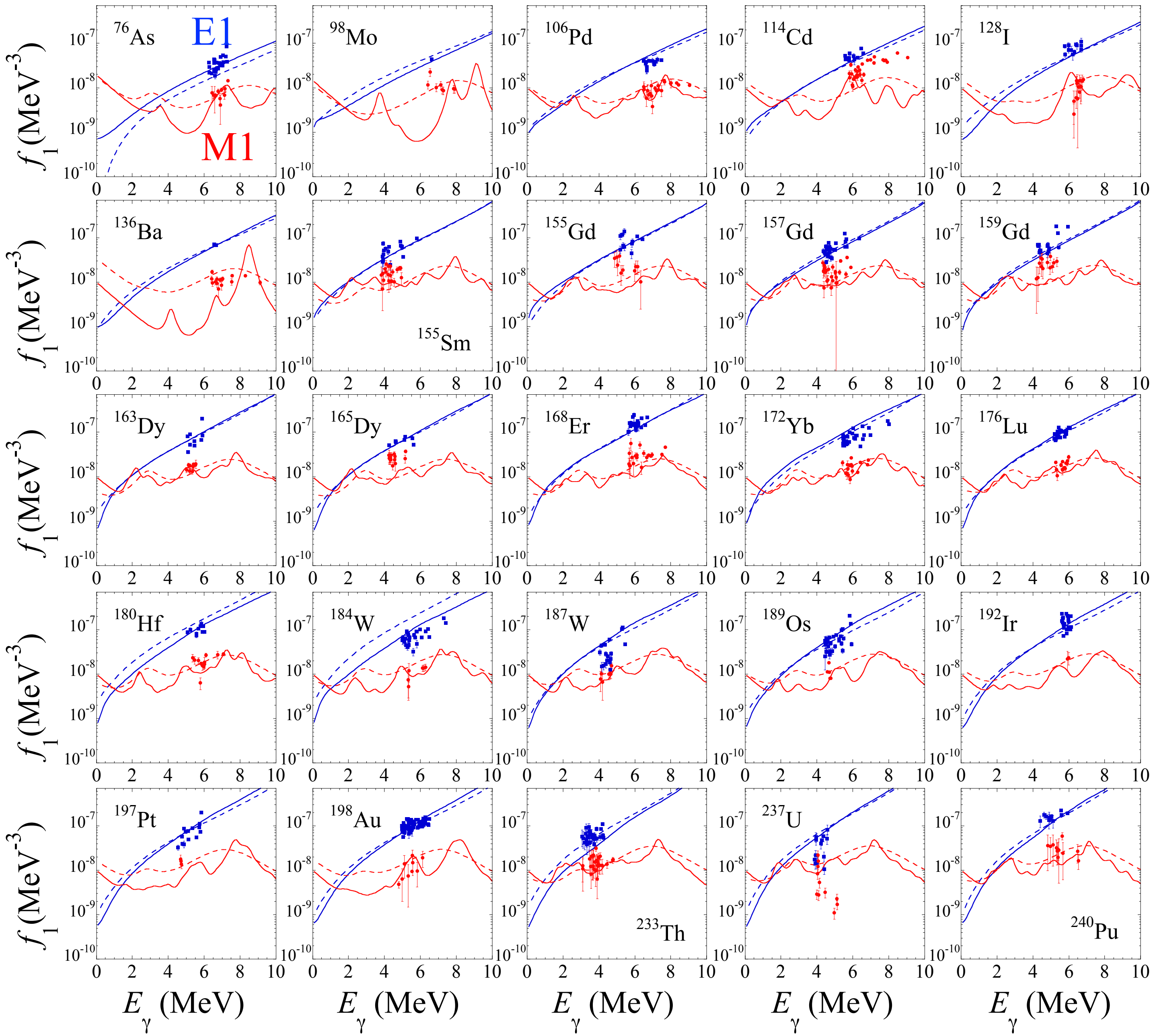

Comparison of D1M+QRPA+0lim and SMLO with Oslo data

30 nuclei out of 72

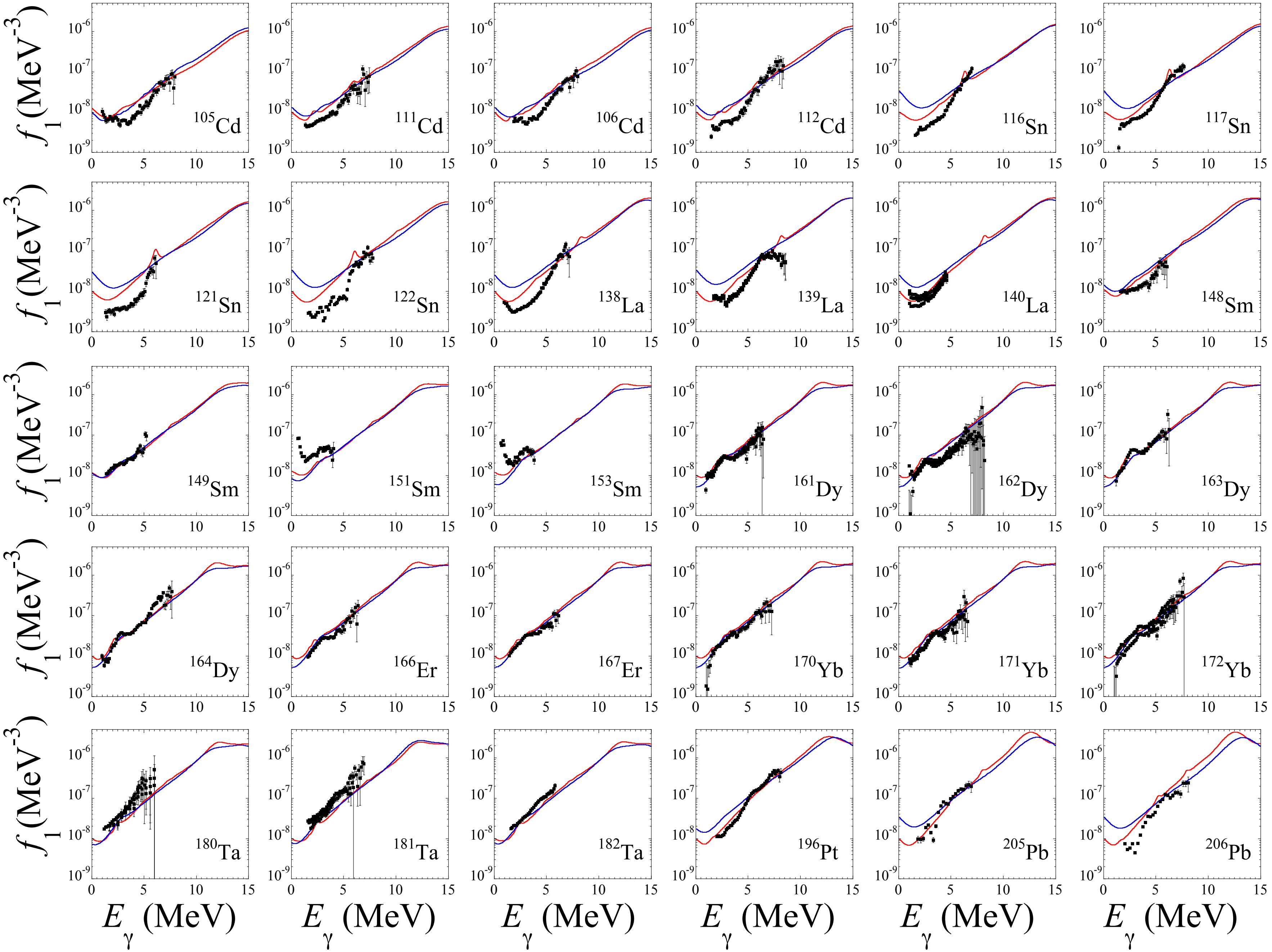

The long-standing problem of the average radiative width $<\Gamma_\gamma>$

$$\langle\Gamma_\gamma\rangle = \frac{D_0}{2\pi}\sum_{X,L,J,\pi}\int_0^{S_n+E_n} T_{XL}(\varepsilon_\gamma)\times\rho(S_n+E_n-\varepsilon_\gamma,J,\pi)d\varepsilon_\gamma$$

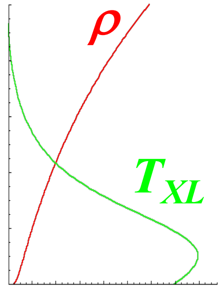

Standard SLO

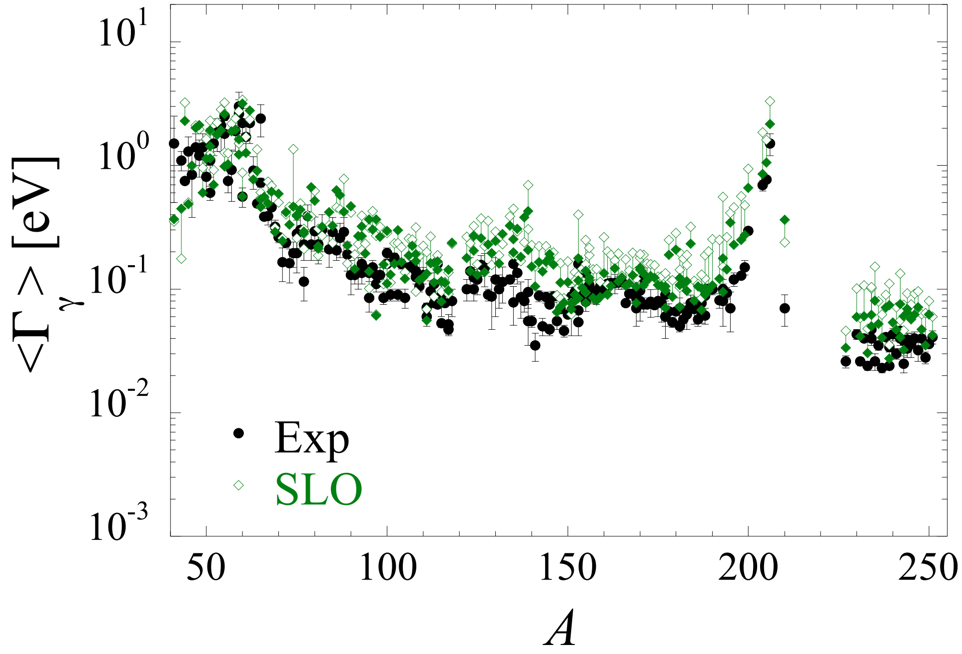

Standard GLO

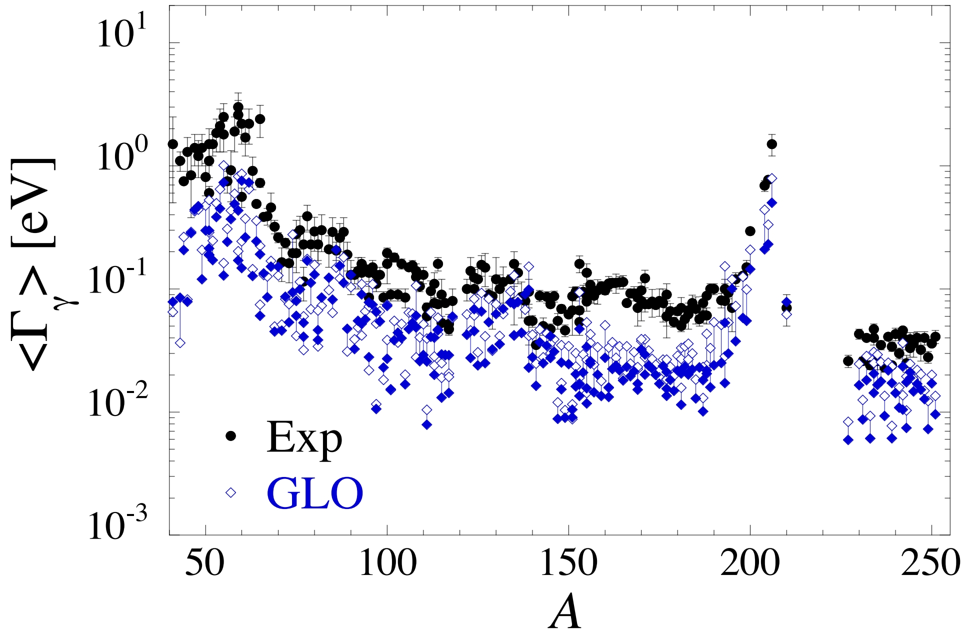

230 nuclei

Full diamonds = CT + BSFG

Open diamonds = HFB + Combinatorial

Comparison of D1M+QRPA+0lim and SMLO with <Γ$_\gamma$> data

$$\langle \Gamma_\gamma \rangle = \frac{D_0}{2\pi} \sum_{X,L,J,\pi} \int_0^{S_n+E_n} T_{XL}(\varepsilon_\gamma) \times \rho(S_n + E_n - \varepsilon_\gamma, J, \pi) d\varepsilon_\gamma$$

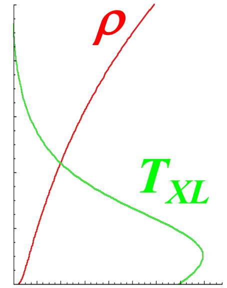

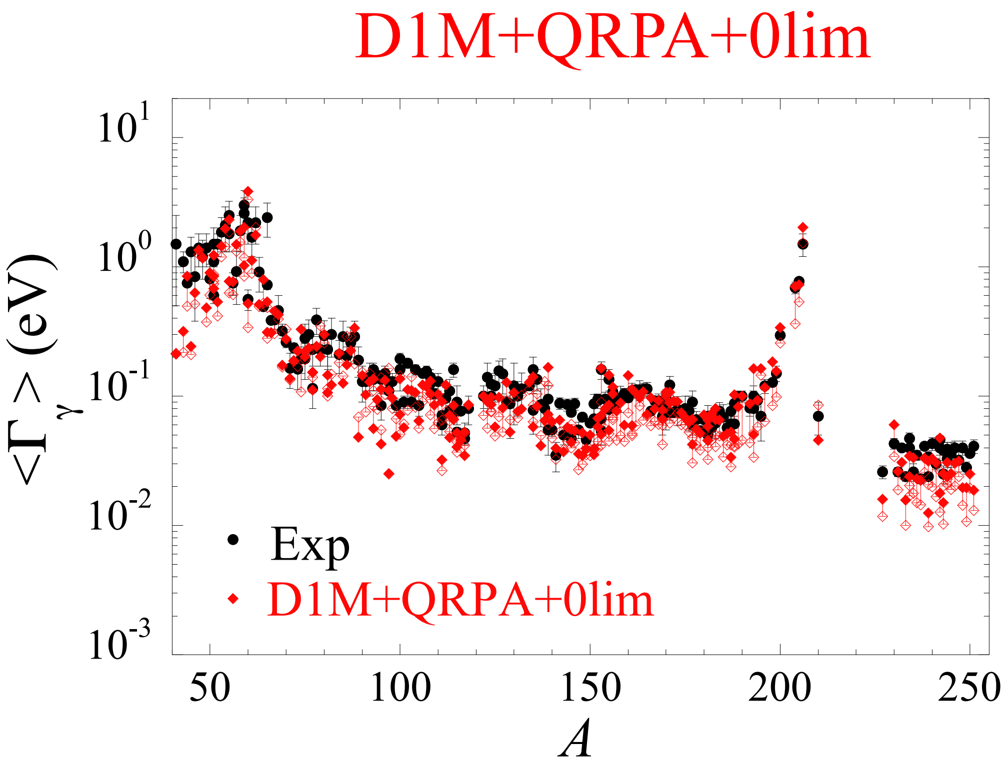

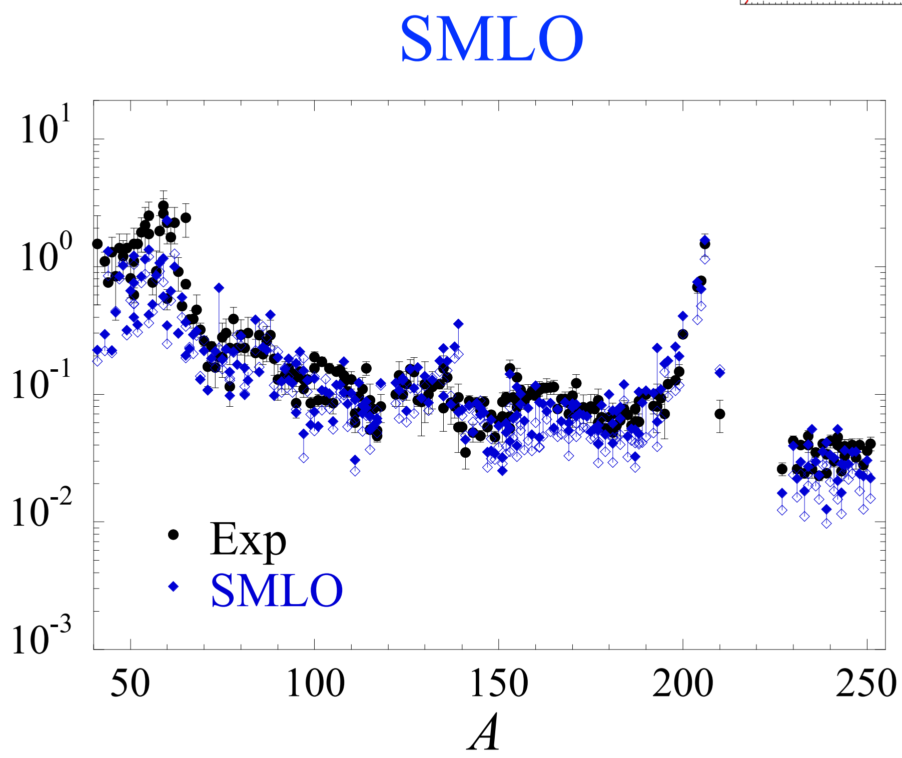

Open diamonds = CT + BSFG
Full diamonds = HFB + Combinatorial

Both PSF models reproduce ~230 <Γ$_\gamma$> within ~ 30-50%

Photon Strength Function

New D1M+QRPA calculations of the **de-excitation** PSF

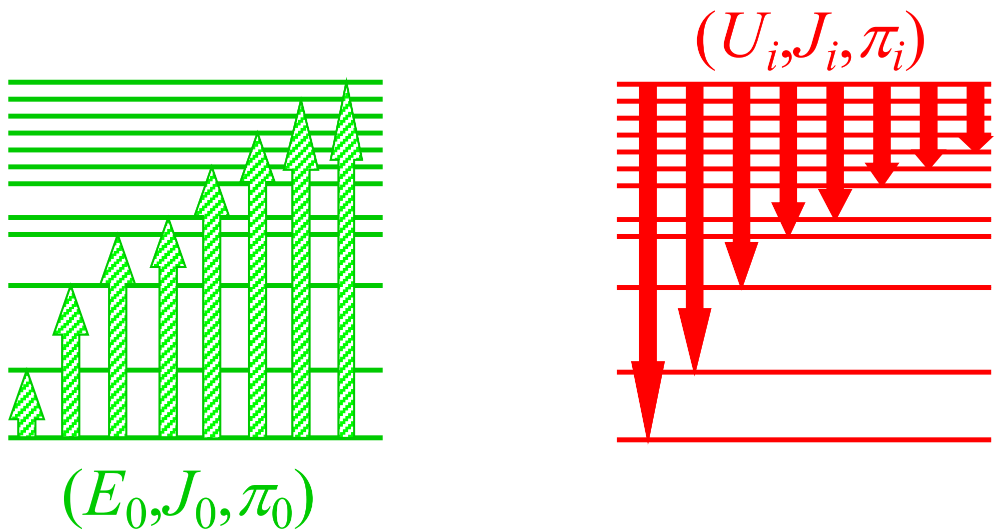

cf Péru's and Hilaire's talk

D1M+QRPA calculation of the de-excitation strength B(XL)

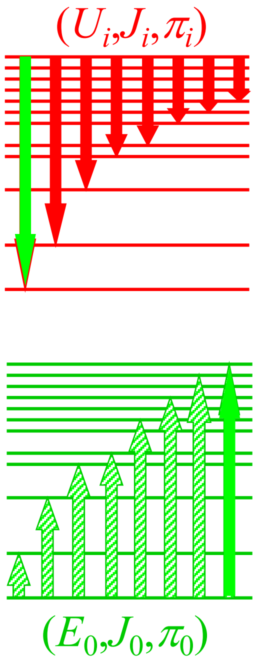

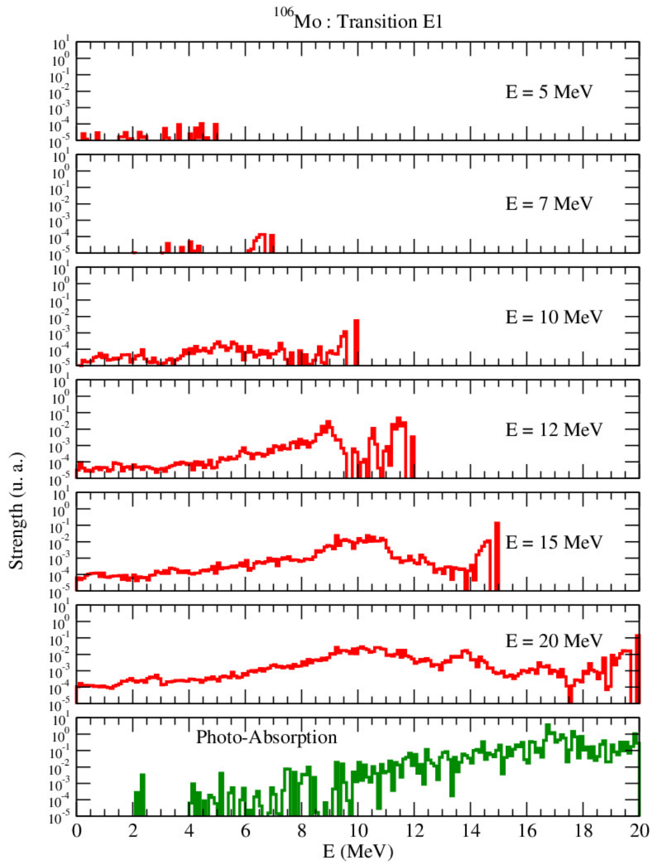

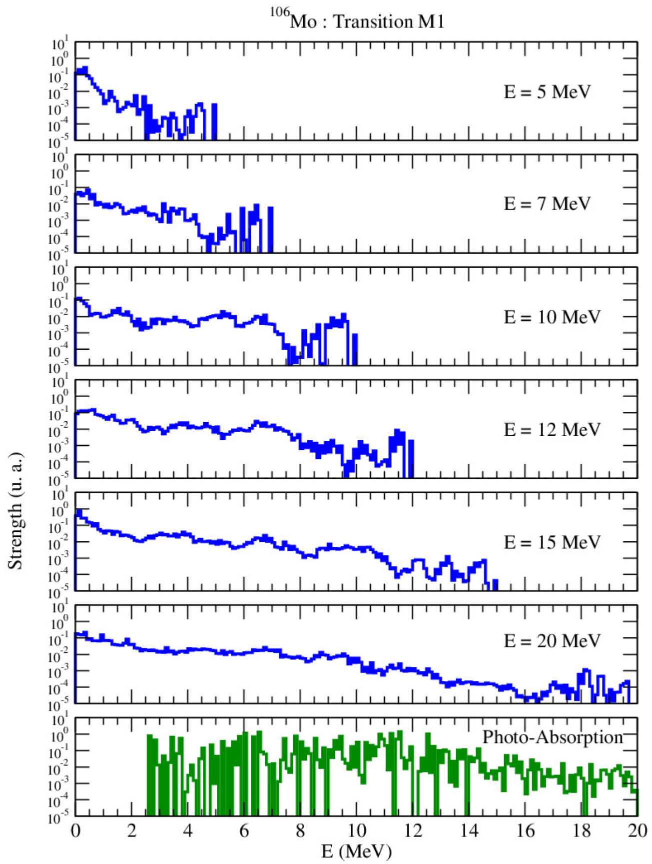

PSF

$$f_{XL}(E_\gamma,U_i)=\sum_{Ji,\pi i} f_{\text{conv}} <B(XL)>(E_\gamma,U_i,J_i,\pi_i)\ \rho(U_i,J_i,\pi_i)$$

De-excitation PSF at an initial energy U_i

$$f_{XL}(E_\gamma, U_i) = \sum_{Ji,\pi i} f_{\text{conv}} \langle B(XL)\rangle(E_\gamma, U_i, J_i, \pi_i)\ \rho(U_i, J_i, \pi_i)$$

Reciprocity theorem

$$\overrightarrow{f_{XL}}(E_\gamma) = \overleftarrow{f_{XL}}(U_i, E_\gamma)$$

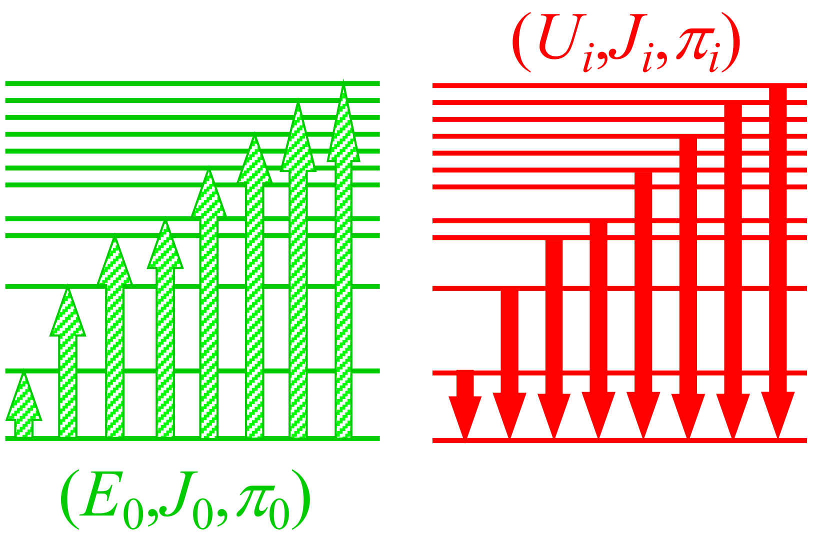

De-excitation PSF at $U_i = E_\gamma$ *after folding* should correspond to the smooth (after folding) photo-absorption PSF at E_γ

f_{E1} de-excitation PSF *before* folding

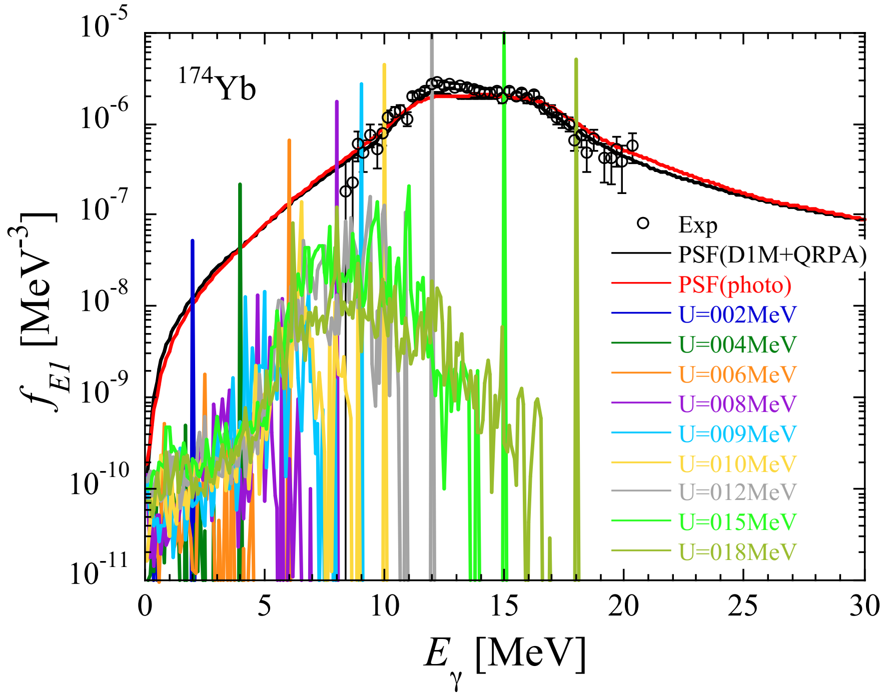

Smooth de-excitation PSF at an initial energy U_i

$$f_{E1}(E) = \int_{-\infty}^{+\infty} L(E,\omega) S_{E1}(\omega)\, d\omega \quad \text{with} \quad L(E,\omega) = \frac{1}{\pi\Gamma} \frac{\Gamma^2 E^2}{\left[E^2 - (\omega-\Delta)^2\right]^2 + \Gamma^2 E^2}$$

$\Delta = 0.14\omega$ & $\Gamma(E1) = 7 - A/45$MeV

f_{E1} de-excitation PSF *before* smoothing

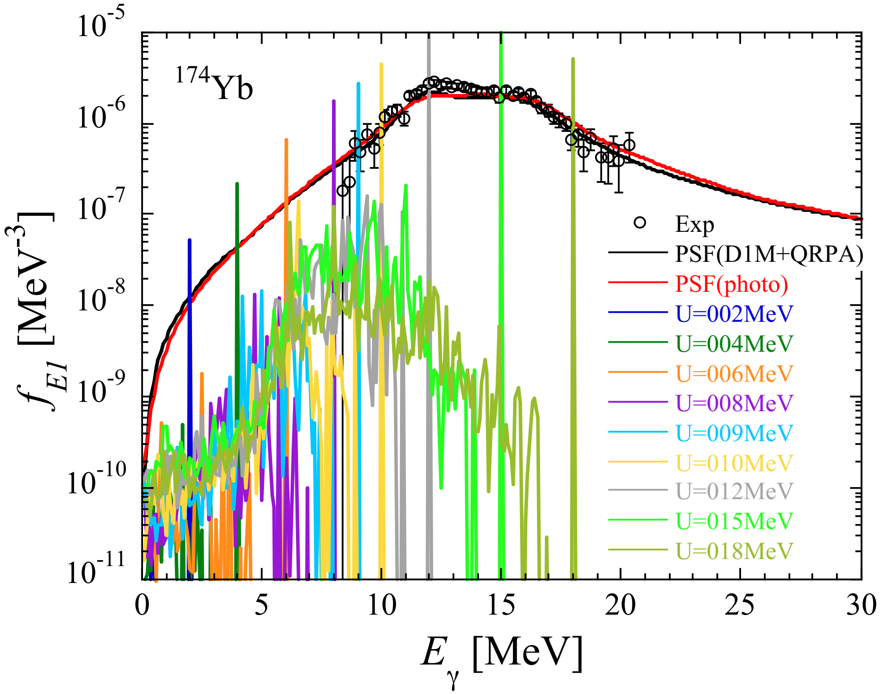

f_{E1} de-excitation PSF *after* smoothing

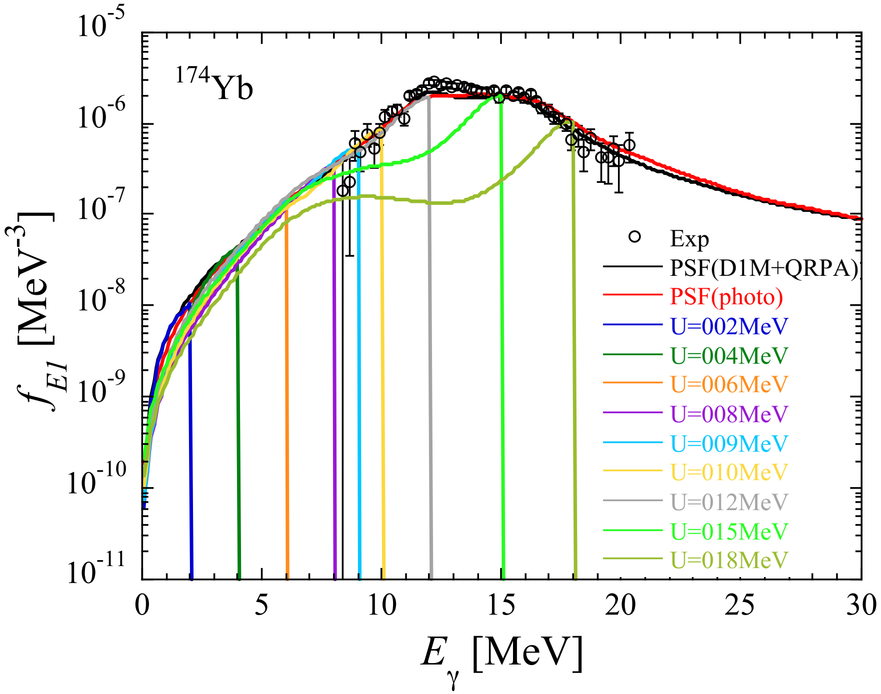

Negligible low-energy
E1 enhancement

Smooth de-excitation PSF at an initial energy U_i

$$f_{E1}(E) = \int_{-\infty}^{+\infty} L(E,\omega) S_{E1}(\omega) d\omega \quad \text{with} \quad L(E,\omega) = \frac{1}{\pi\Gamma} \frac{\Gamma^2 E^2}{\left[E^2 - (\omega - \Delta)^2\right]^2 + \Gamma^2 E^2}$$

$\Delta = 0.14\omega$ & $\Gamma = 1$MeV

f_{M1} de-excitation PSF *before* smoothing

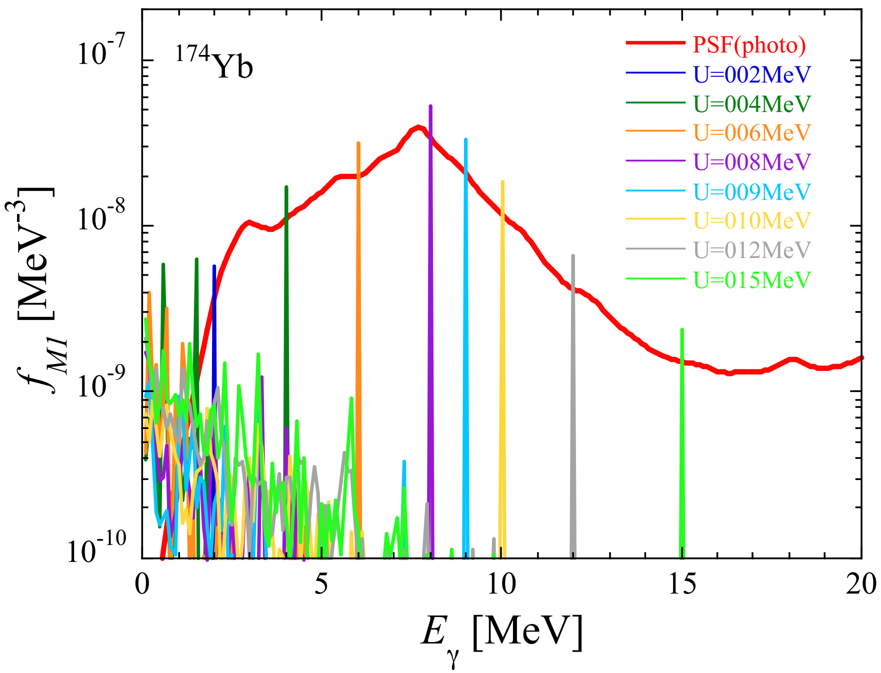

f_{M1} de-excitation PSF *after* smoothing

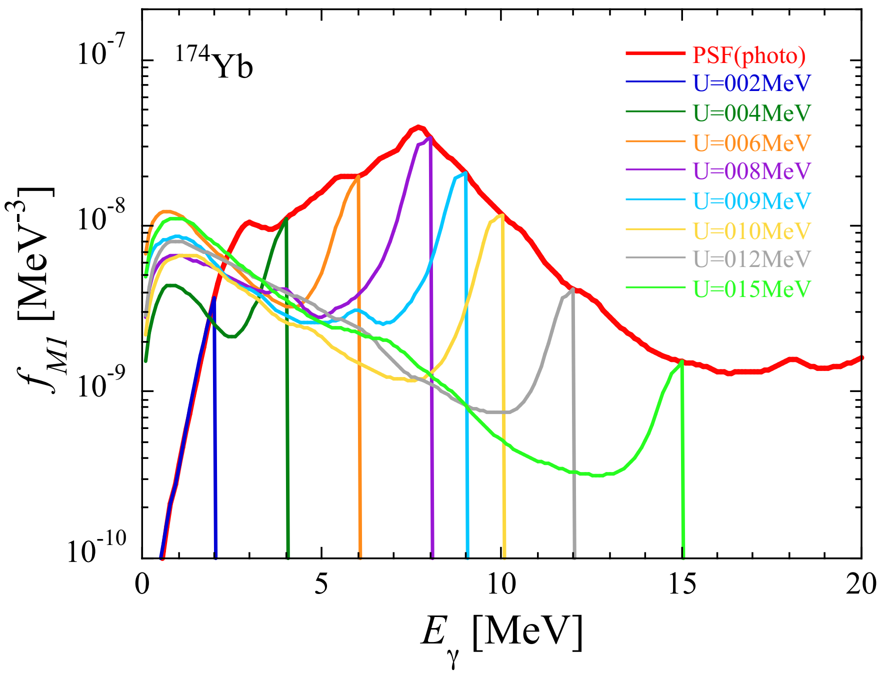

Significant low-energy
M1 enhancement

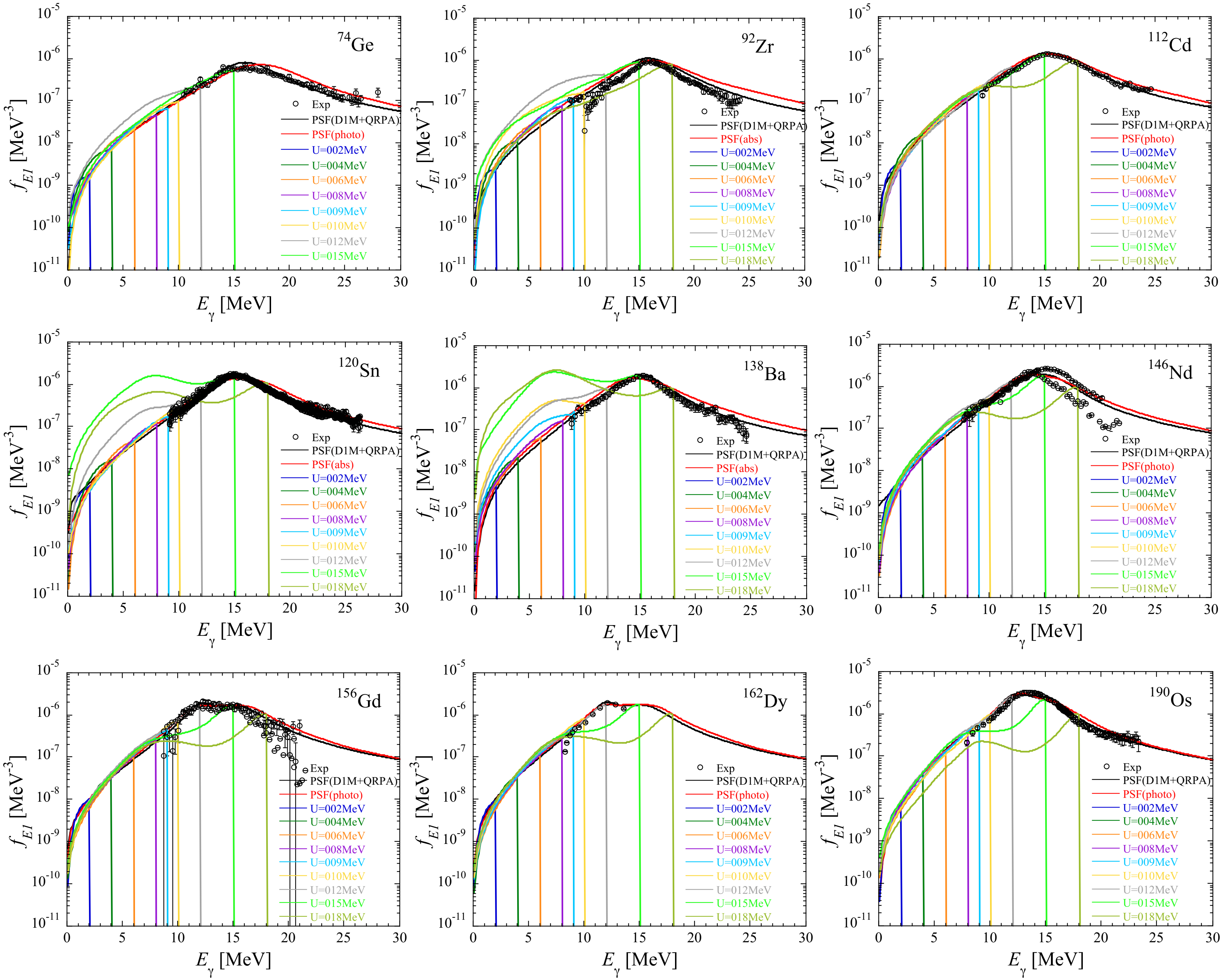

^{74}Ge
Exp
PSF(D1M+QRPA)
PSF(photo)
U=002MeV
U=004MeV
U=006MeV
U=008MeV
U=009MeV
U=010MeV
U=012MeV
U=015MeV
^{92}Zr
Exp
PSF(D1M+QRPA)
PSF(abs)
U=002MeV
U=004MeV
U=006MeV
U=008MeV
U=009MeV
U=010MeV
U=012MeV
U=015MeV
U=018MeV
^{112}Cd
Exp
PSF(D1M+QRPA)
PSF(photo)
U=002MeV
U=004MeV
U=006MeV
U=008MeV
U=009MeV
U=010MeV
U=012MeV
U=015MeV
U=018MeV
^{120}Sn
Exp
PSF(D1M+QRPA)
PSF(abs)
U=002MeV
U=004MeV
U=006MeV
U=008MeV
U=009MeV
U=010MeV
U=012MeV
U=015MeV
U=018MeV
^{138}Ba
Exp
PSF(D1M+QRPA)
PSF(abs)
U=002MeV
U=004MeV
U=006MeV
U=008MeV
U=009MeV
U=010MeV
U=012MeV
U=015MeV
U=018MeV
^{146}Nd
Exp
PSF(D1M+QRPA)
PSF(photo)
U=002MeV
U=004MeV
U=006MeV
U=008MeV
U=009MeV
U=010MeV
U=012MeV
U=015MeV
U=018MeV
^{156}Gd
Exp
PSF(D1M+QRPA)
PSF(photo)
U=002MeV
U=004MeV
U=006MeV
U=008MeV
U=009MeV
U=010MeV
U=012MeV
U=015MeV
U=018MeV
^{162}Dy
Exp
PSF(D1M+QRPA)
PSF(photo)
U=002MeV
U=004MeV
U=006MeV
U=008MeV
U=009MeV
U=010MeV
U=012MeV
U=015MeV
U=018MeV
^{190}Os
Exp
PSF(D1M+QRPA)
PSF(photo)
U=002MeV
U=004MeV
U=006MeV
U=008MeV
U=009MeV
U=010MeV
U=012MeV
U=015MeV
U=018MeV
f_{E1} [MeV^{-3}]
E_γ [MeV]

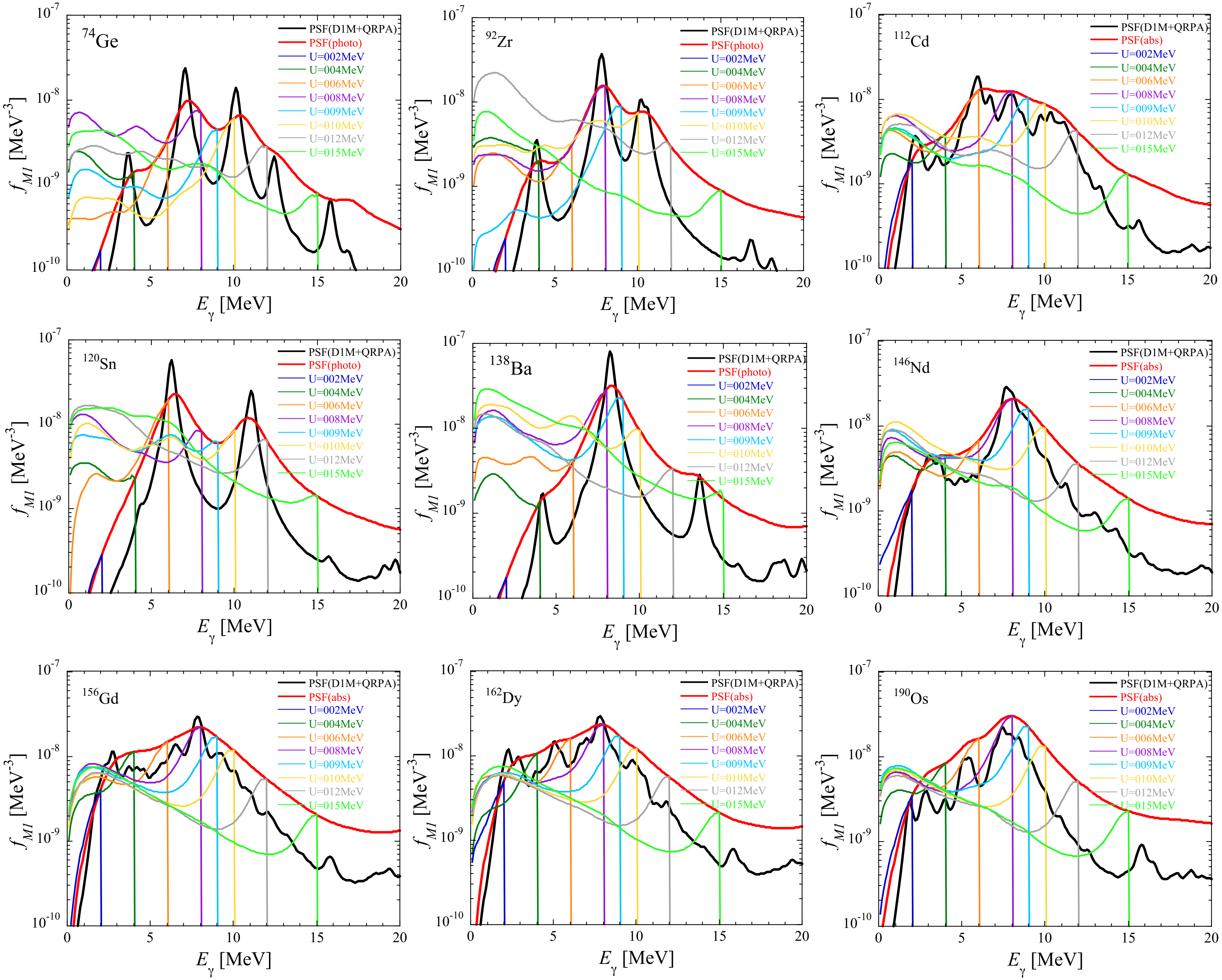

74Ge
92Zr
112Cd
120Sn
138Ba
146Nd
156Gd
162Dy
190Os
PSF(D1M+QRPA)
PSF(photo)
PSF(abs)
U=002MeV
U=004MeV
U=006MeV
U=008MeV
U=009MeV
U=010MeV
U=012MeV
U=015MeV
f_M1 [MeV^-3]
E_γ [MeV]
10^-7
10^-8
10^-9
10^-10
0
5
10
15
20

QRPA de-excitation PSF at an initial energy U_i

$$f_{E1}(E) = \int_{-\infty}^{+\infty} L(E,\omega) S_{E1}(\omega) d\omega \quad \text{with}$$

$$L(E,\omega) = \frac{1}{\pi\Gamma} \frac{\Gamma^2 E^2}{\left[E^2 - (\omega-\Delta)^2\right]^2 + \Gamma^2 E^2}$$

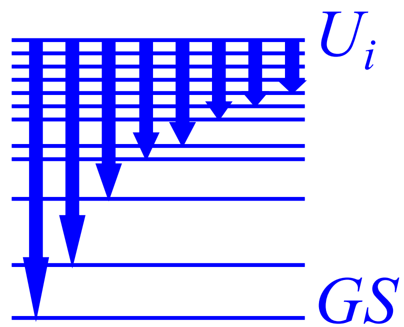

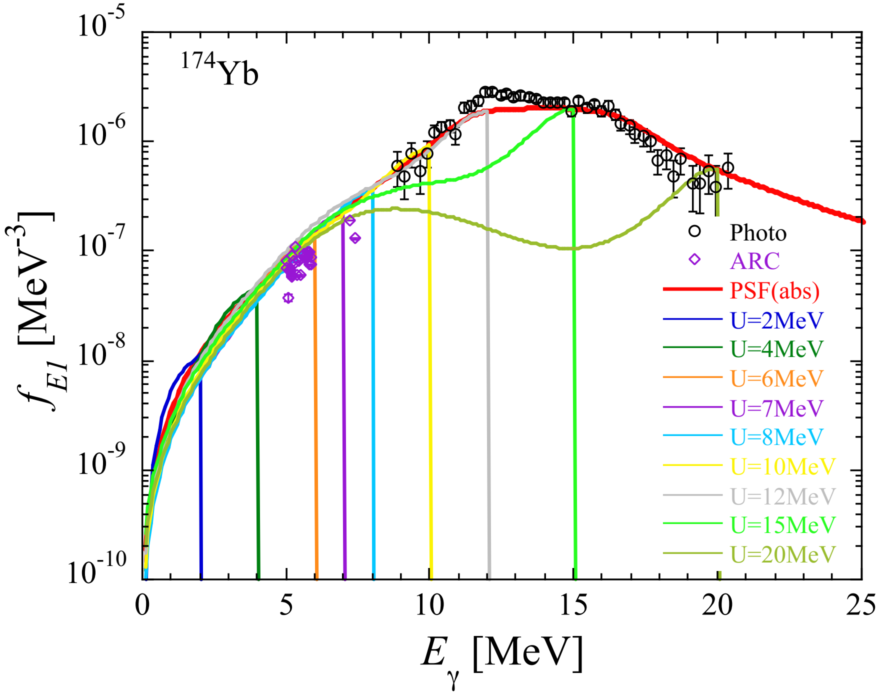

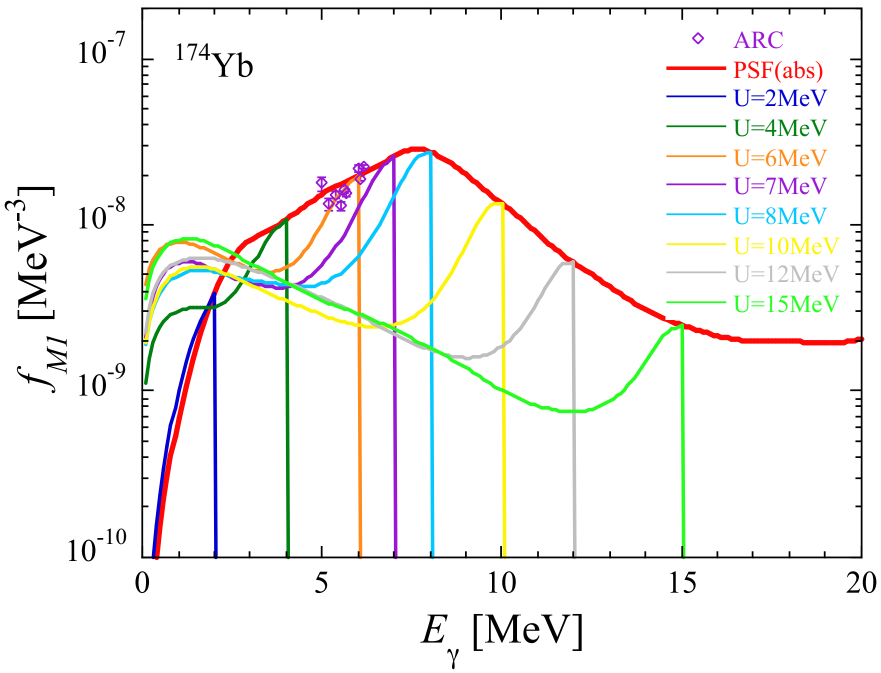

Negligible low-energy E1 enhancement

For M1: significant

- enhancement at $E_\gamma < 2$MeV
- reduction at 2MeV $< E_\gamma < U$

→ impact on low-S_n n-capture

Impact of the de-excitation PSF on radiative n-capture cross sections

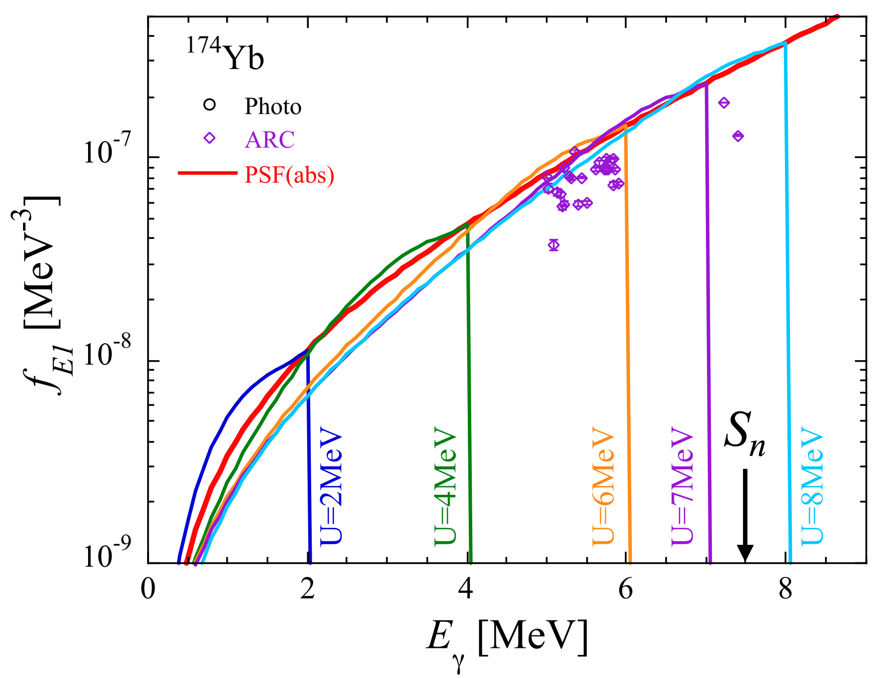

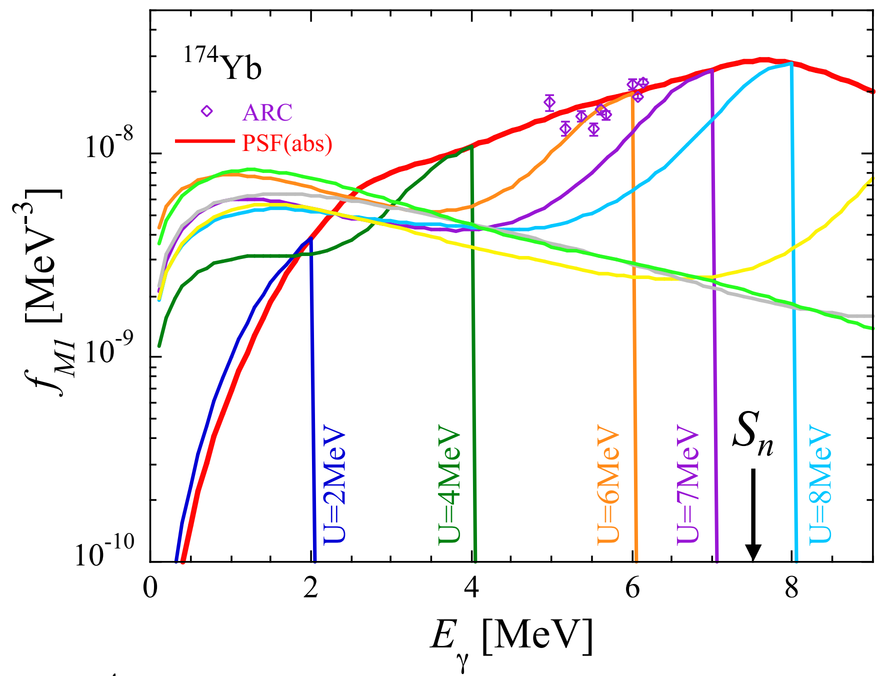

Decrease of the (n,γ) cross section when including the de-excitation PSF with respect to the photo-absorption PSF

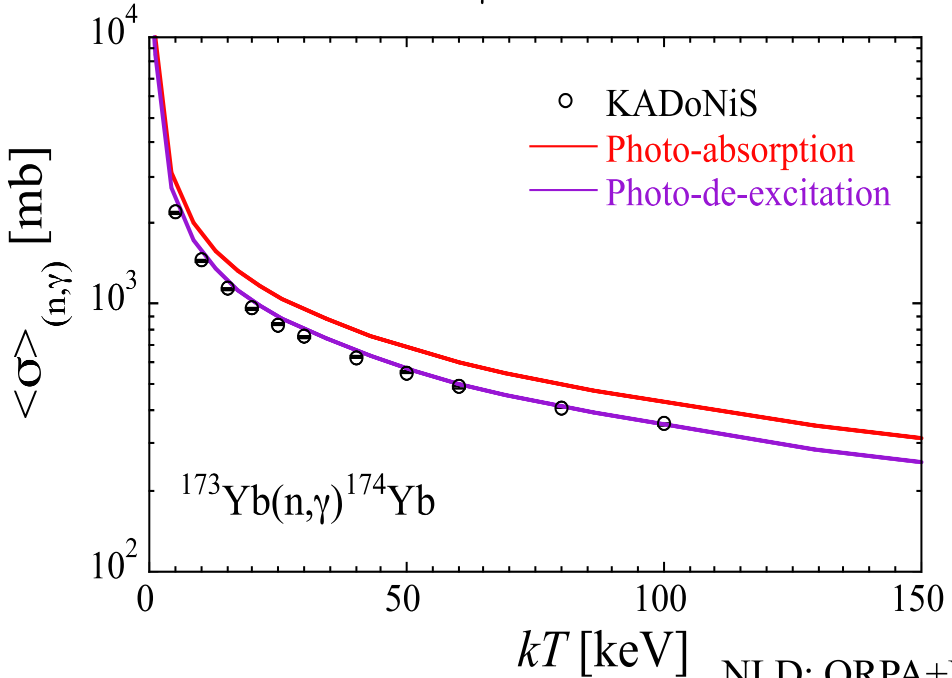

NLD: QRPA+BE

Predicted de-excitation E1 PSF as a function of excitation energy for a given E_γ

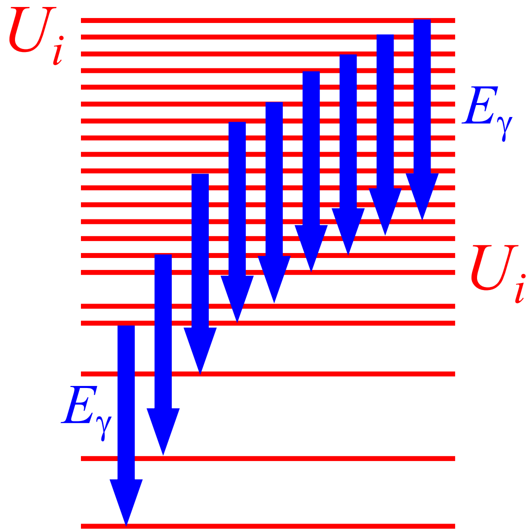

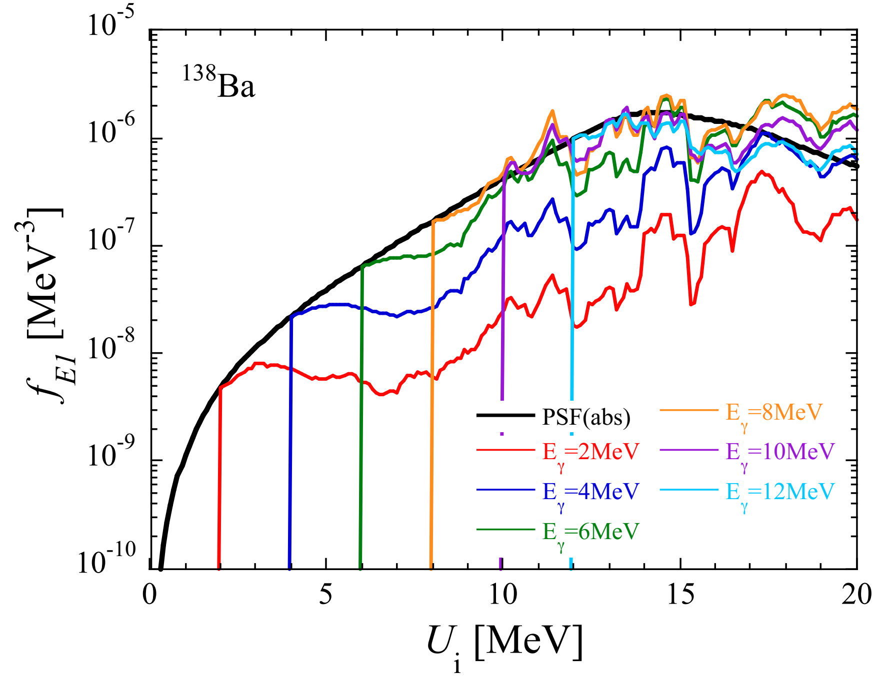

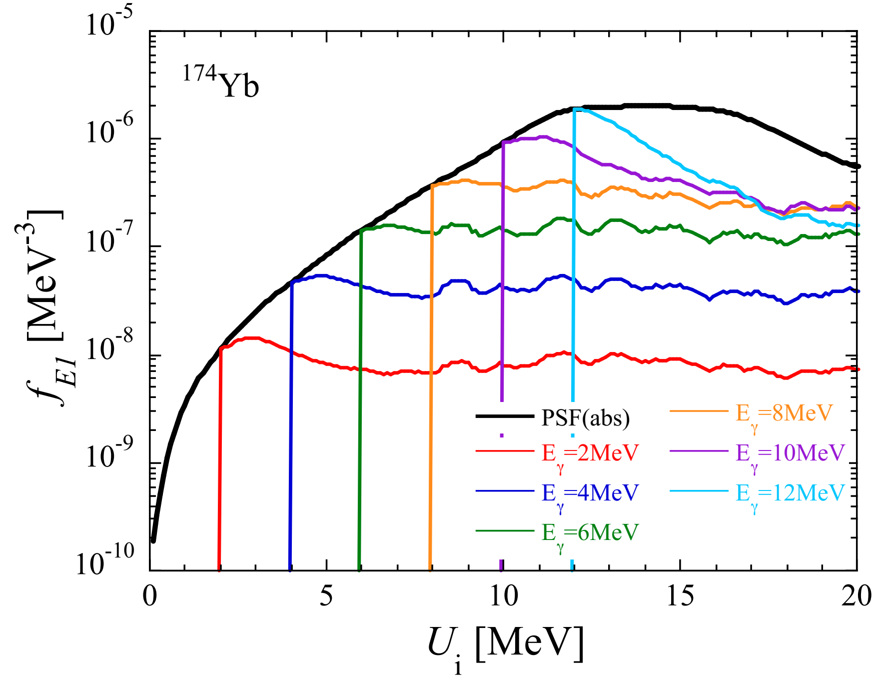

Predicted de-excitation M1 PSF as a function of excitation energy for a given E_γ

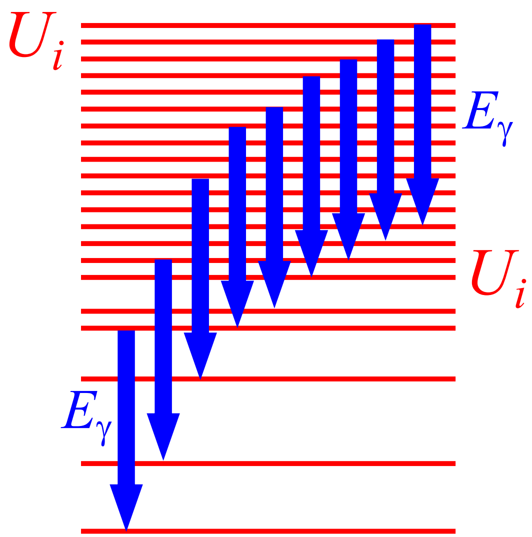

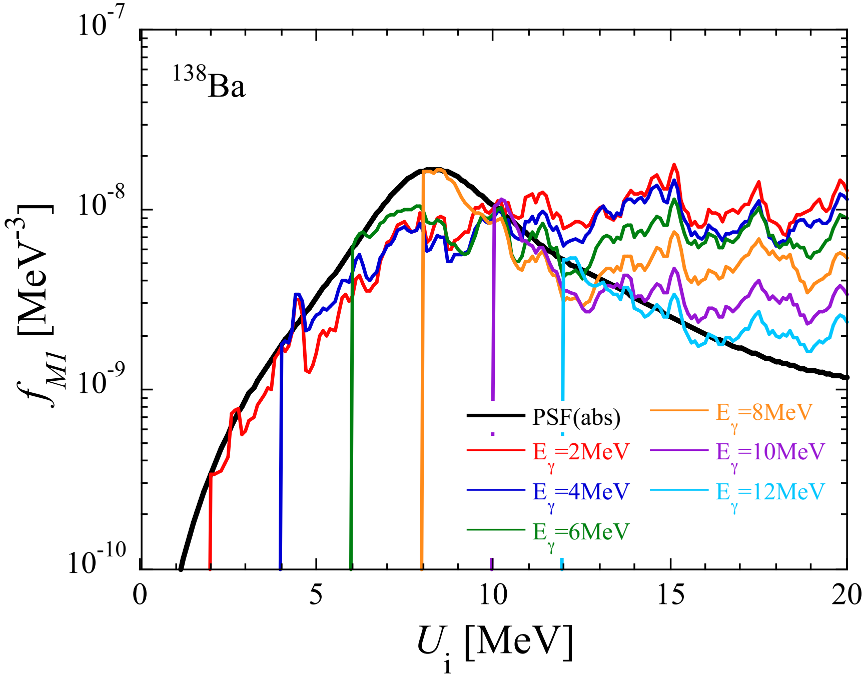

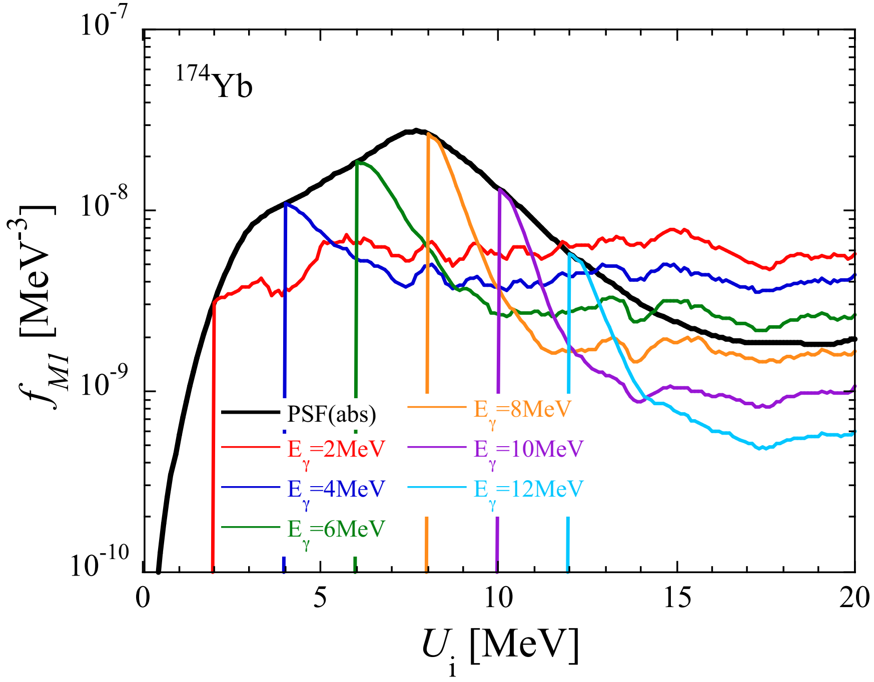

$\langle \mathrm{PSF}(U<S_\mathrm{n}) \rangle$: average $\langle f_{\mathrm{E1+M1}}(E_\gamma) \rangle$ over different initial excitation energies $U_i<S_n$

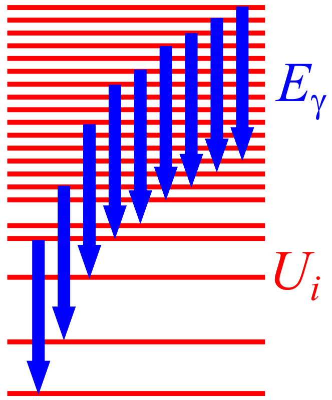

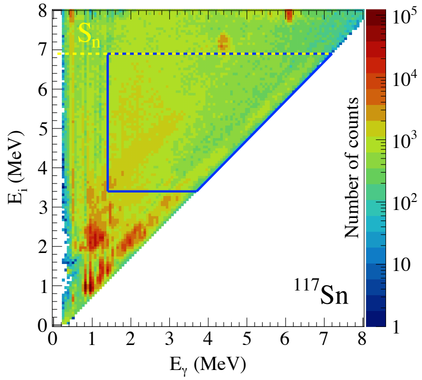

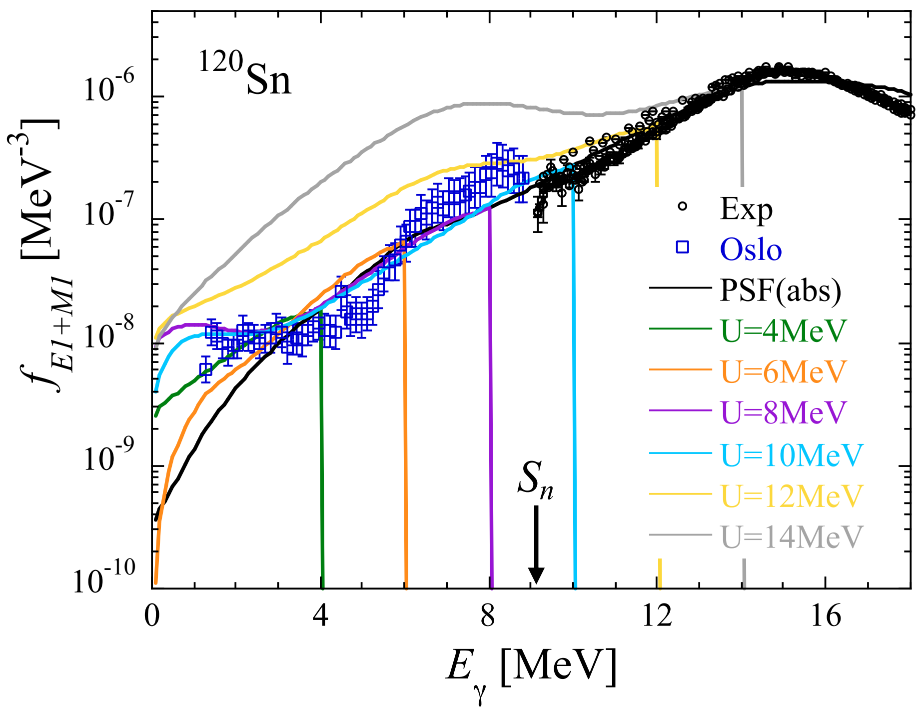

$\langle \mathrm{PSF}(U<S_\mathrm{n})\rangle$: average $\langle f_{\mathrm{E1+M1}}(E_\gamma)\rangle$ over different initial excitation energies $U_\mathrm{i}<S_\mathrm{n}$

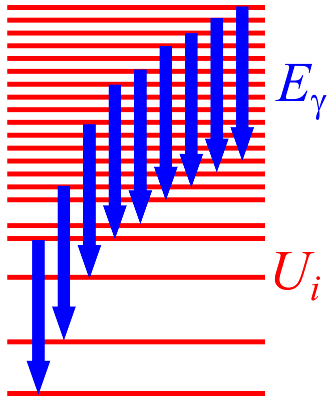

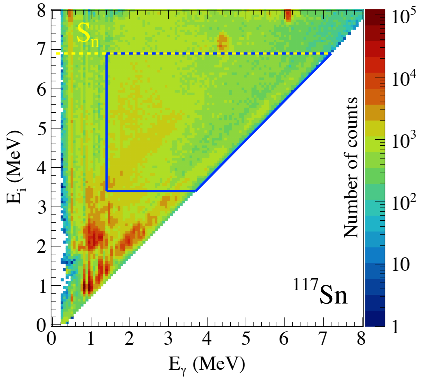

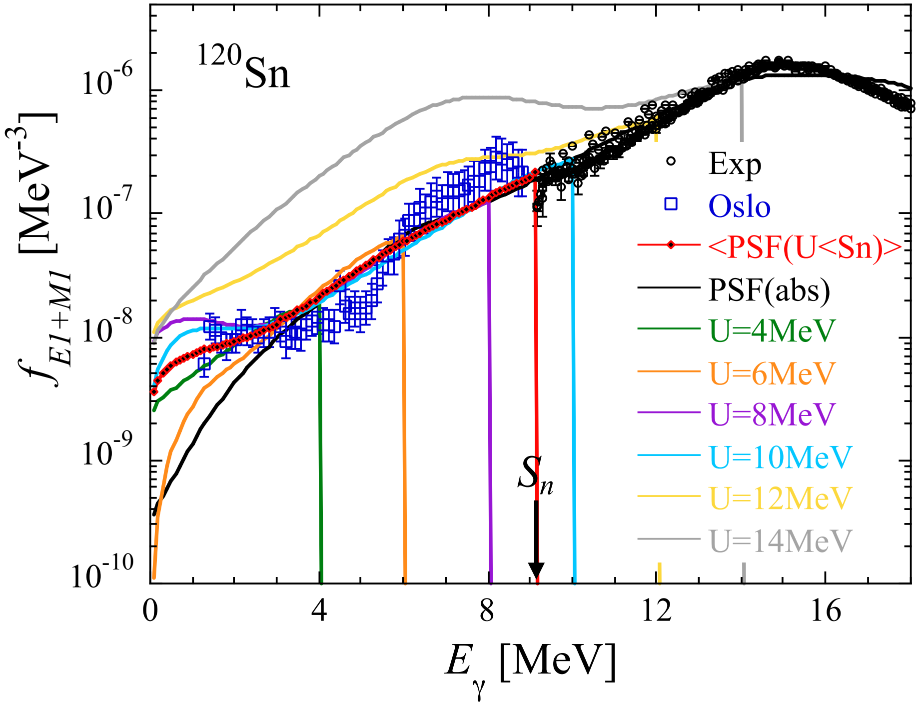

<PSF(U<S_n)>: average <$f_{E1+M1}(E_\gamma)$> over different initial excitation energies U_i<S_n

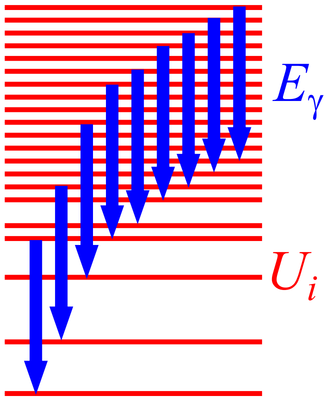

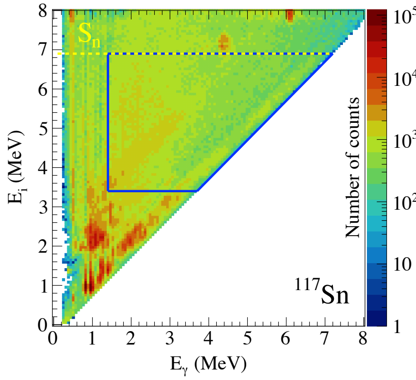

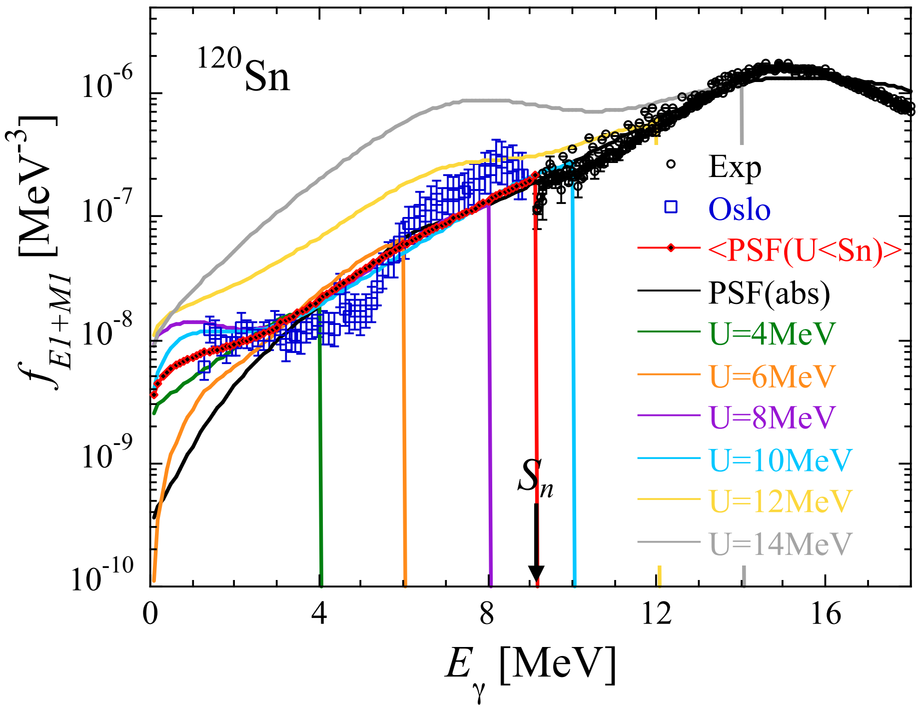

Impact of the low-energy PSF on (n,γ) cross section

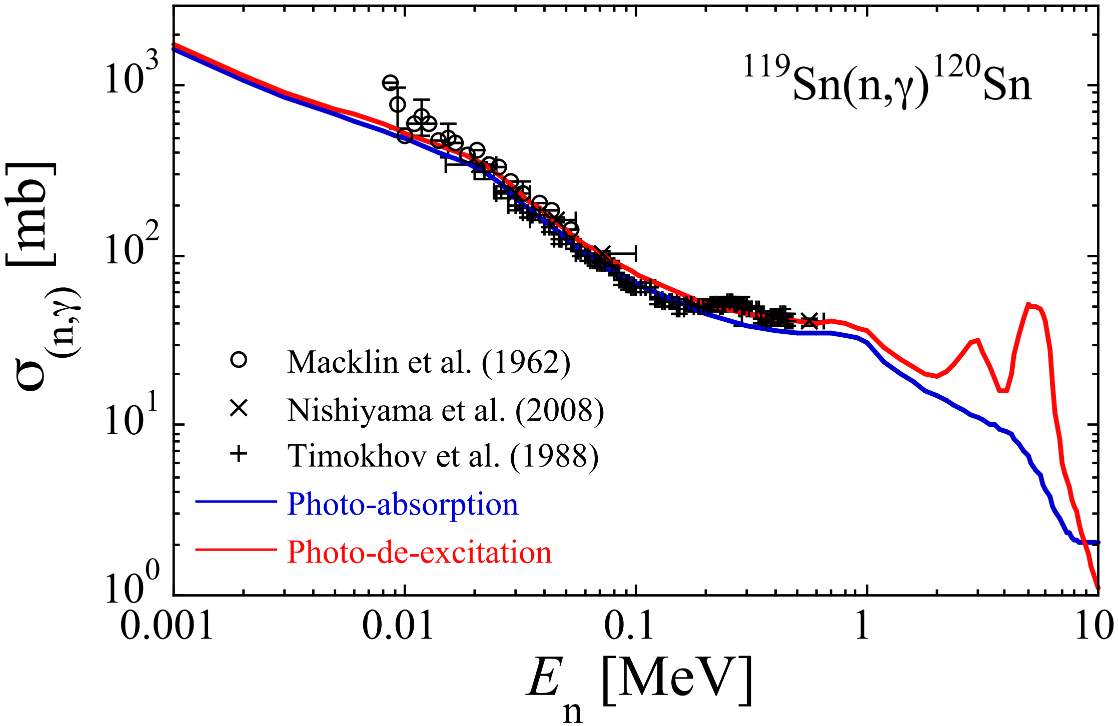

Significant impact on (n,γ) cross section at E_n>2MeV (E_γ>11MeV)

Lack of (n,γ) data in the MeV region for spherical nuclei

Comparison of D1M+QRPA (de-exc) with <Γ$_\gamma$> data

$$\langle\Gamma_\gamma\rangle = \frac{D_0}{2\pi}\sum_{X,L,J,\pi}\int_0^{S_n+E_n} T_{XL}(\varepsilon_\gamma)\times\rho(S_n+E_n-\varepsilon_\gamma,J,\pi)\,d\varepsilon_\gamma$$

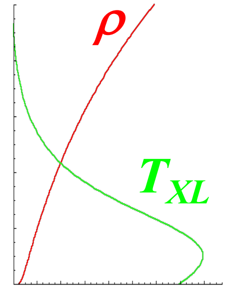

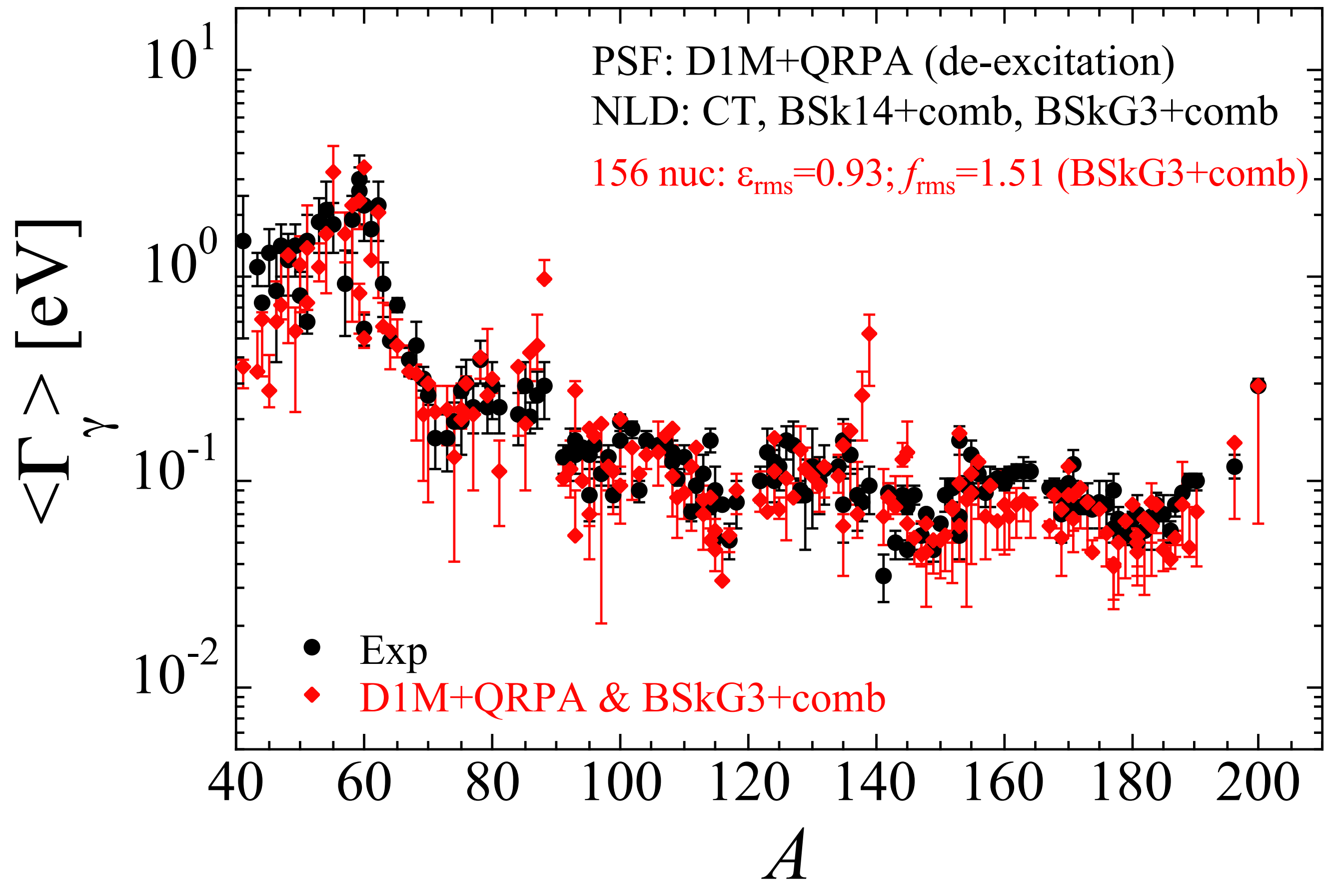

Comparison of D1M+QRPA (de-exc) with MACS data

PSF: D1M+QRPA de-excitation
NLD: BSkG3+combinatorial

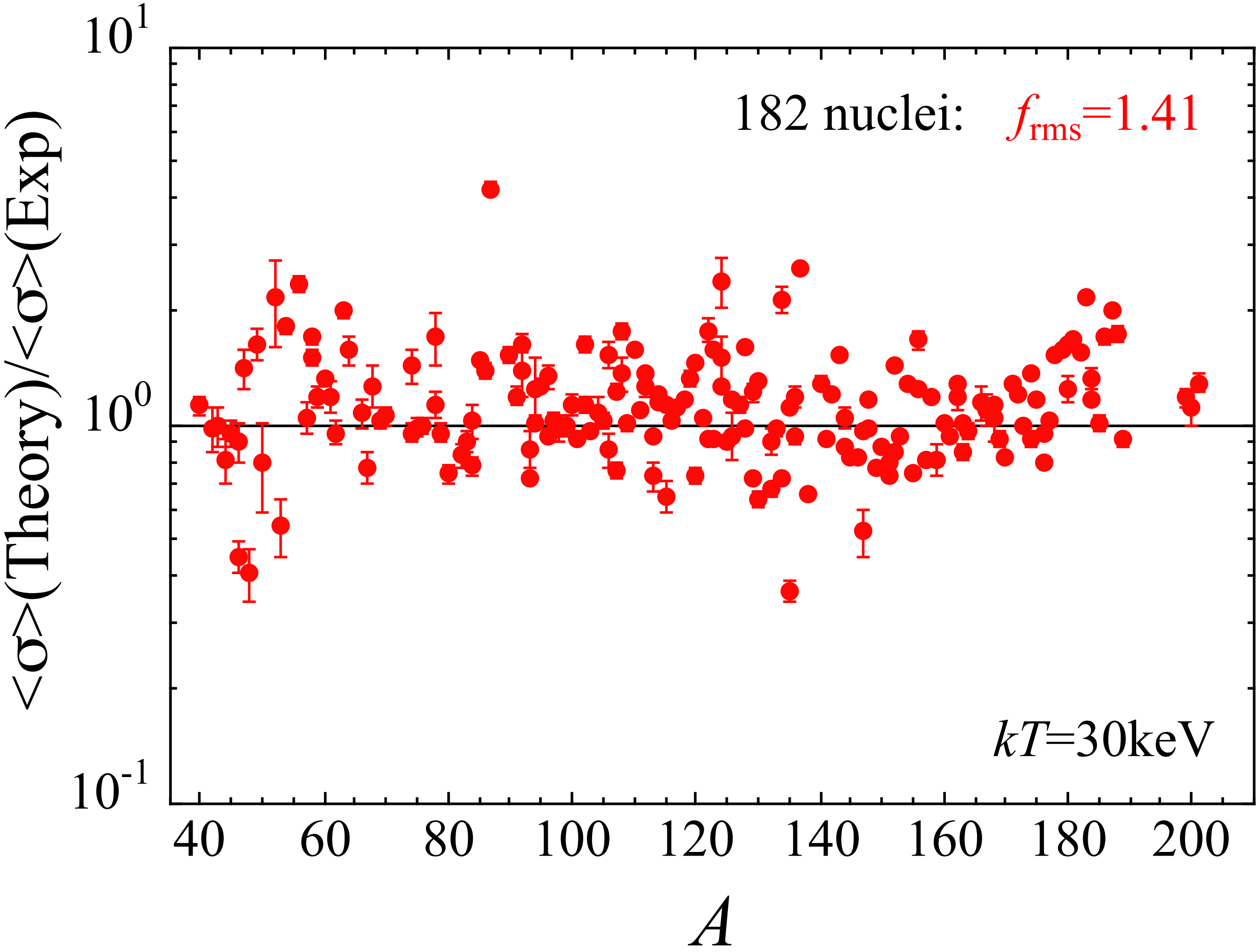

Comparison of D1M+QRPA: de-exc vs abs with MACS data

PSF: D1M+QRPA de-excitation vs absorption
NLD: BSkG3+combinatorial

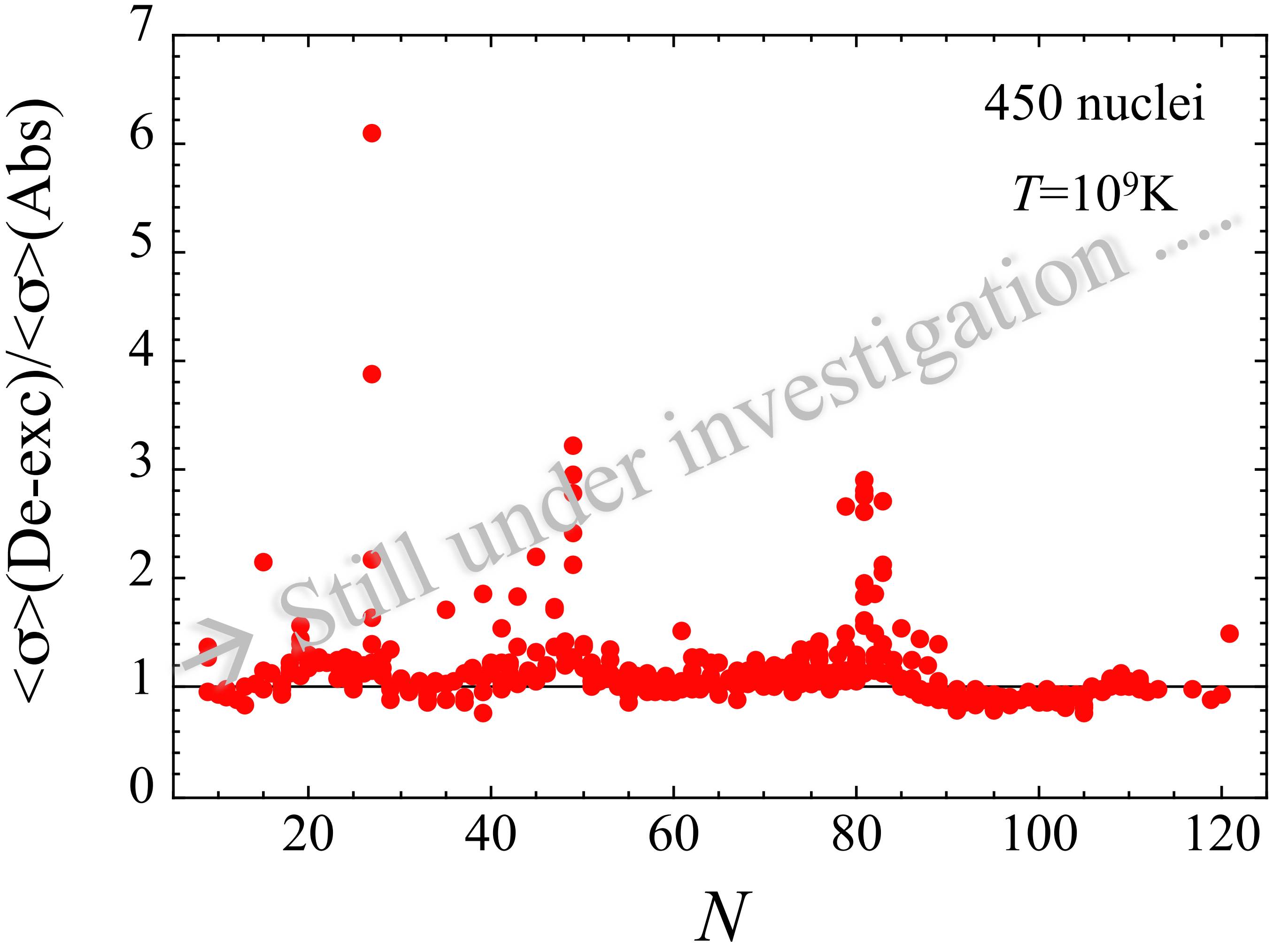

Many nuclear needs including PSF & NLD for the various nucleosynthesis processes

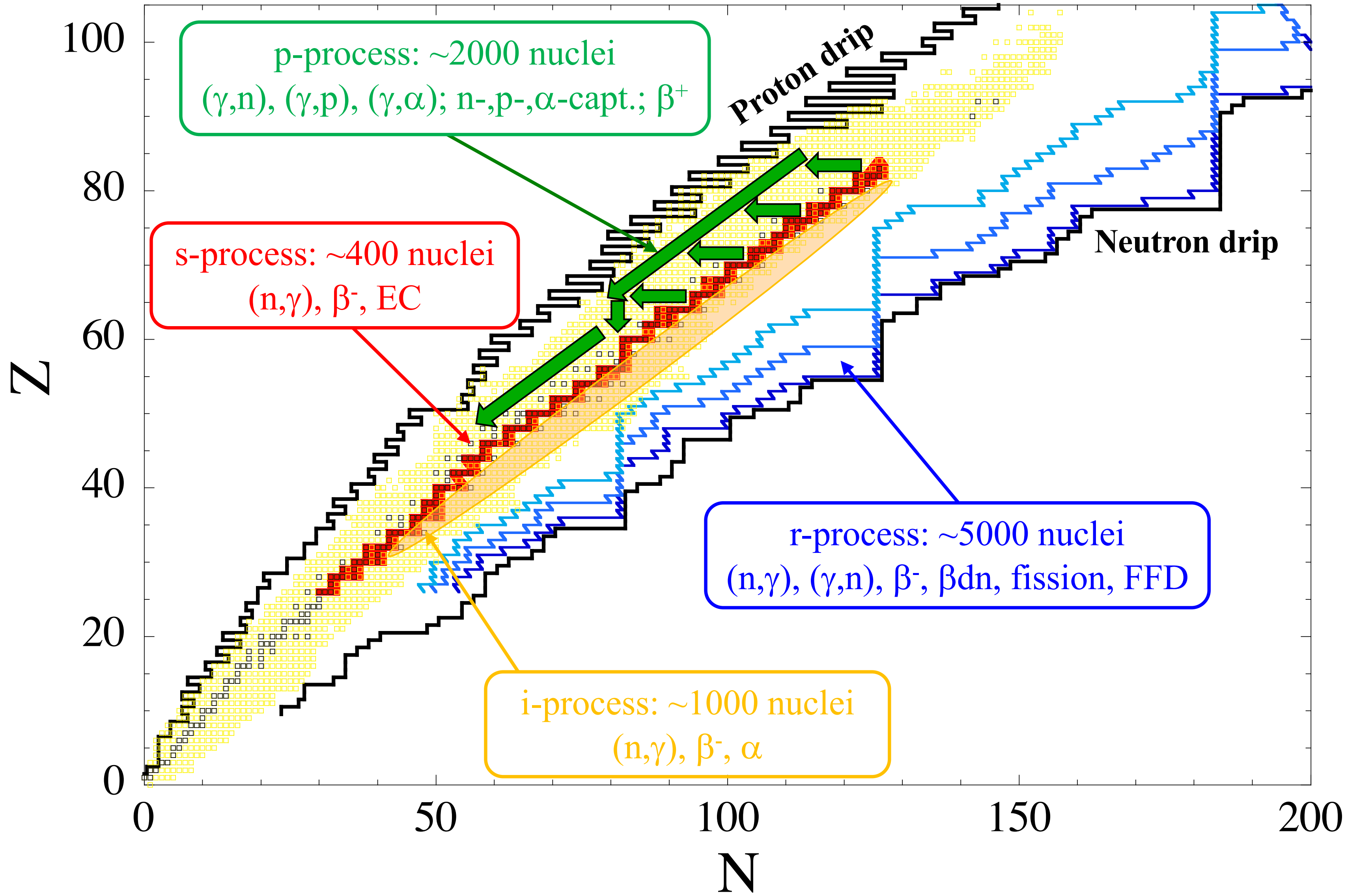

How do PSF and NLD affect astrophysics observables ?

Model and Parameter uncertainties associated with PSF

Experimental data

- Photoabsorption data
- ARC/DRC/Oslo/NRF data
- $<\Gamma_\gamma>$, MSC, MACS data

Models

- Standard Lorentzian
- Modified Lorentzian (GLO, SMLO)
- Skyrme-HFB+QRPA
- Gogny-HFB+QRPA
- RMF+RRPA
- (Beyond QRPA / Shell Model)

Parameter adjustment

- Analytical: GR (E_0 Γ_0 σ_0), ...
- Tables: *etable, ftable, wtable*

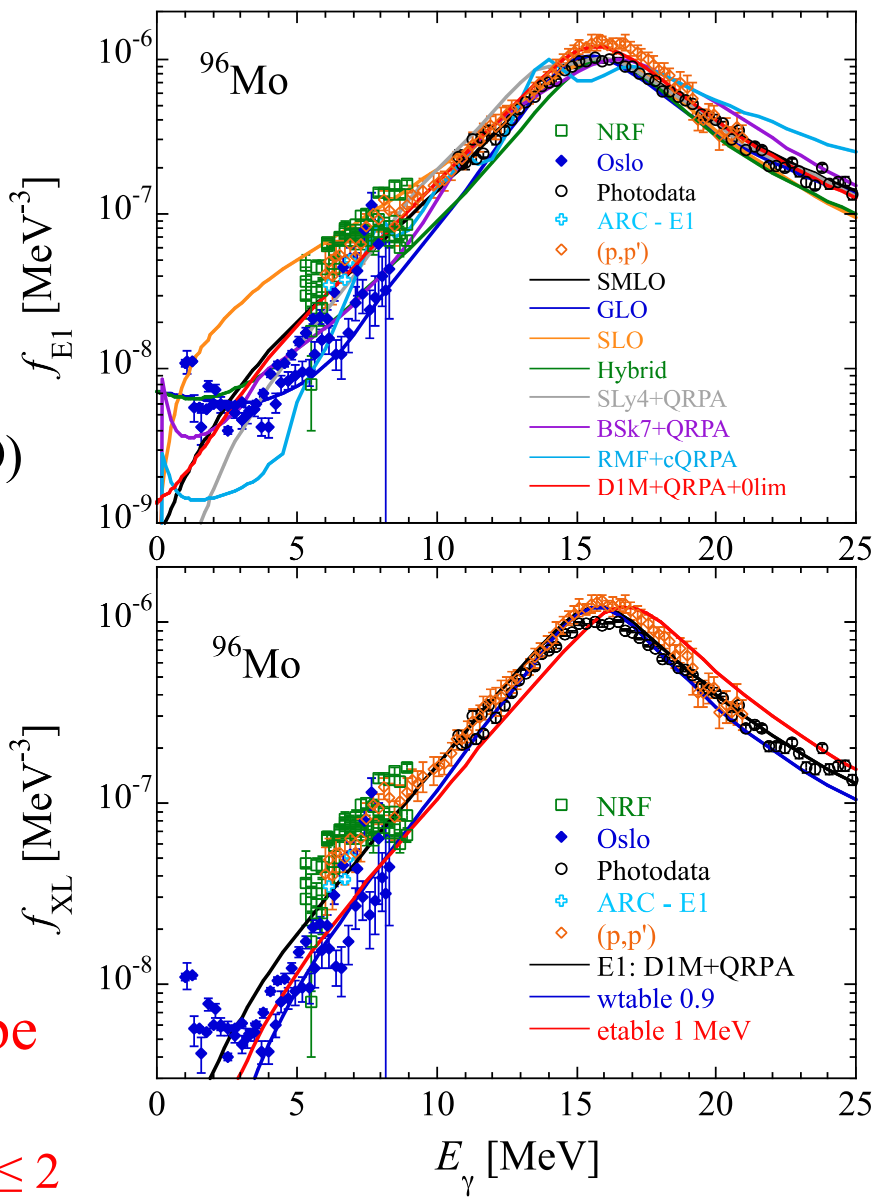

Model and parameter variations must be constrained by experimental data

PSF data as well as (n,γ) cross sections with $f_{rms} \leq 2$

Model and Parameter uncertainties associated with PSF

Experimental data

- Photoabsorption data
- ARC/DRC/Oslo/NRF data
- $<\Gamma_\gamma>$, MSC, MACS data

Models

- ~~Standard Lorentzian~~
- Modified Lorentzian (~~GLO~~, SMLO)
- Skyrme-HFB+QRPA
- Gogny-HFB+QRPA
- RMF+RRPA
- Beyond QRPA / Shell Model

Parameter adjustment

- Analytical: GR (E_0 Γ_0 σ_0), ...
- Tables: *etable, ftable, wtable*

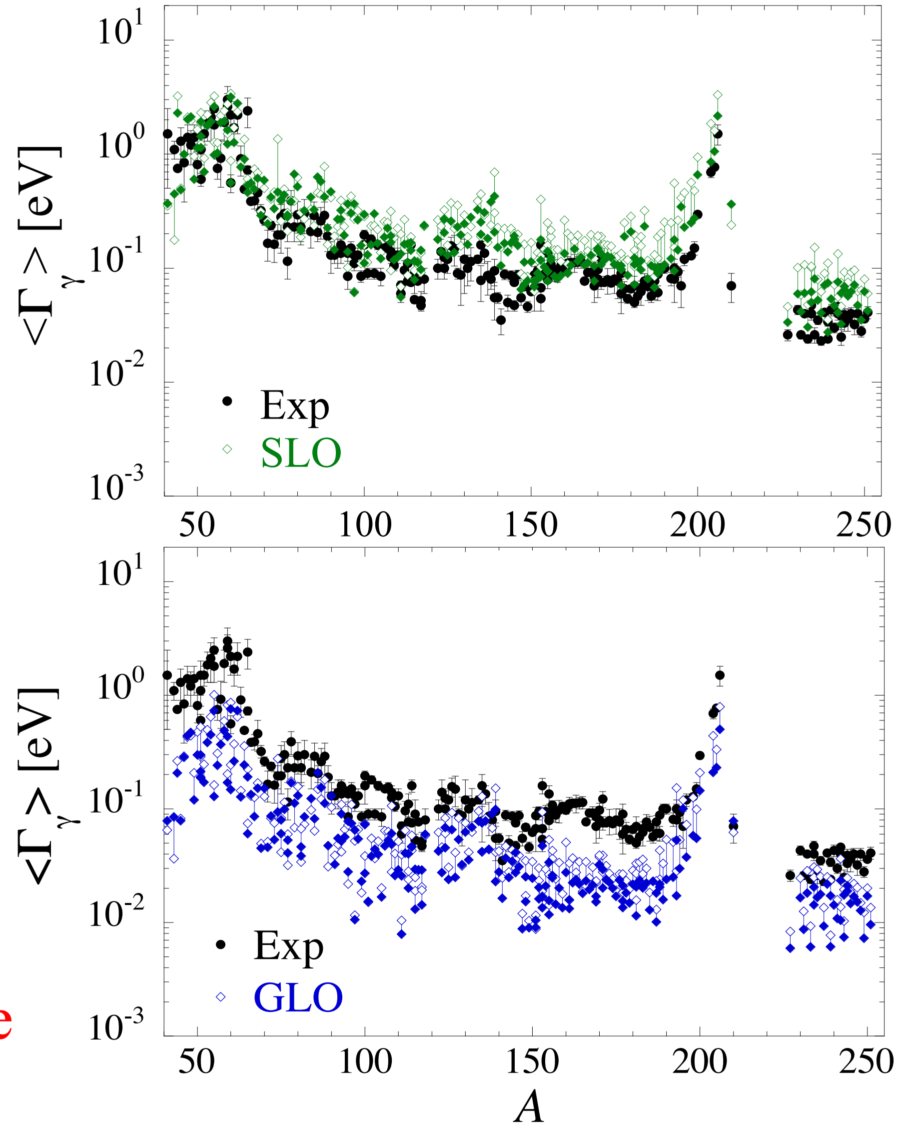

Model and parameter variations must be constrained by experimental data

PSF data as well as (n,γ) cross sections with $f_{\rm rms} \leq 2$

TALYS prediction of the 240 experimental (n,γ) MACS

$20 \leq Z \leq 83$

Correlated model uncertainties

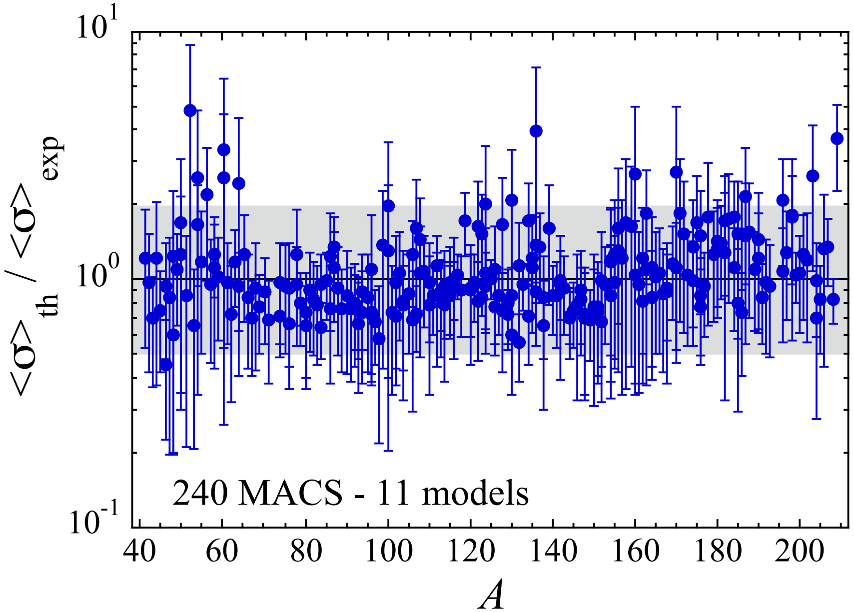

Uncorrelated parameter uncertainties

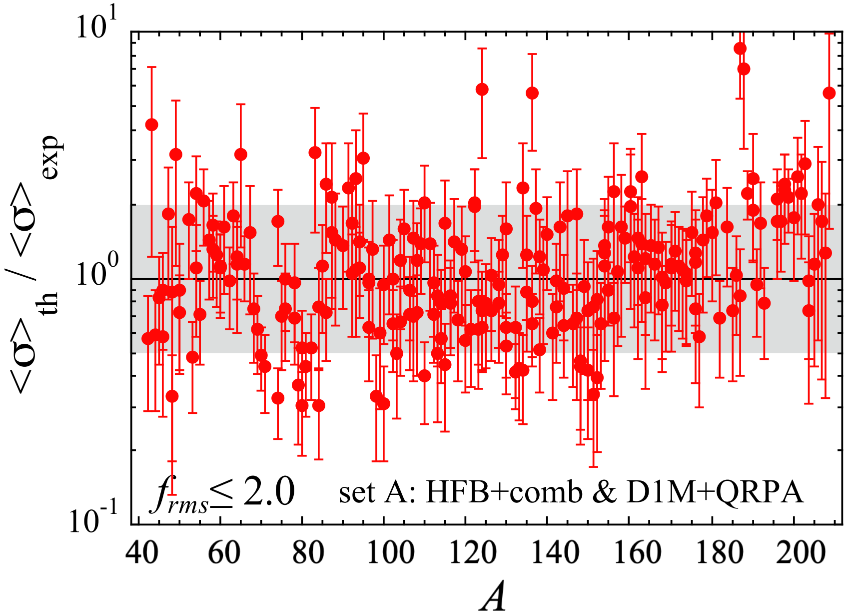

- Experimental info on M, NLD, PSF
- 11 different models of NLD, PSF (Inclusion or not of DC)
- All with $f_{rms} \leq 1.4 - 2.0$

- Experimental masses
- NLD: Cst-T (E_0 & T)
- PSF: SMLO (Γ & ΔE)
- BFMC: 4-par. variation s.t. $f_{rms} \leq 2.0$

Propagation of PSF uncertainties to "realistic" nucleosynthesis models

Impact of on the i-process nucleosynthesis in low-*M* low-*Z* AGB stars

Correlated model uncertainties

NLD

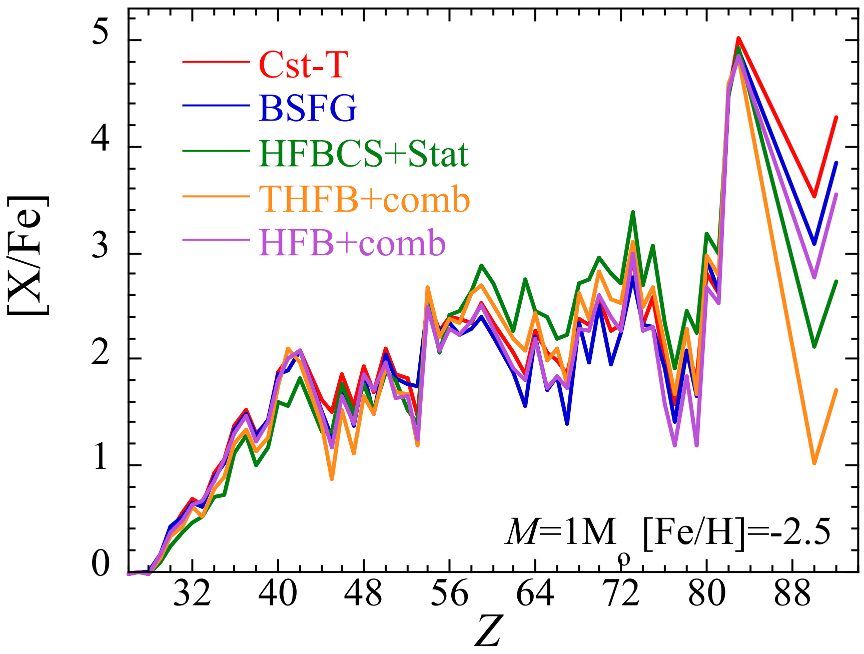

PSF

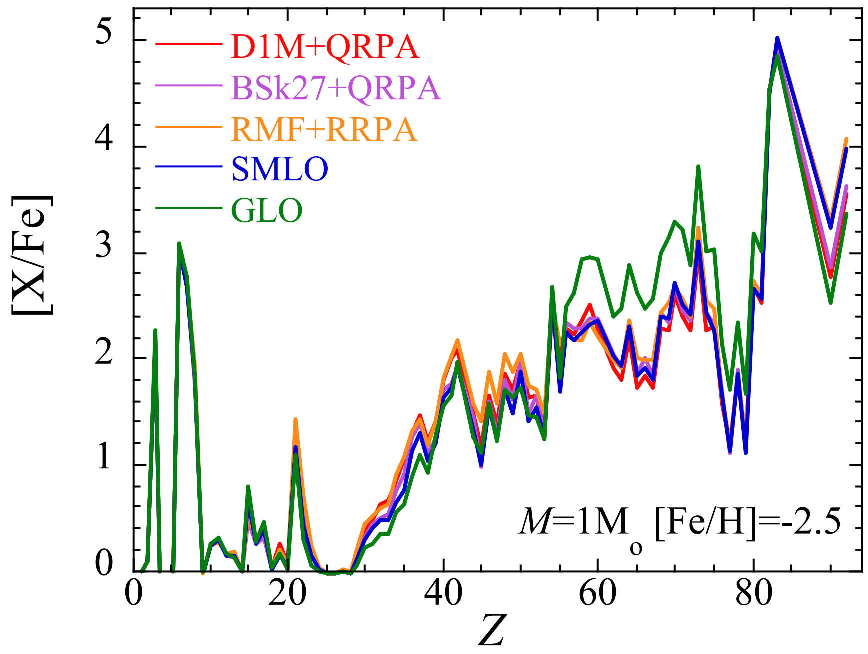

Reduction of the model uncertainties through

- Improved models of NLD & PSF (reject unreliable ones, e.g GLO)
- Experimental constraints on specific rates

Impact of on the i-process nucleosynthesis in low-*M* low-*Z* AGB stars

Uncorrelated PSF & NLD parameter uncertainties

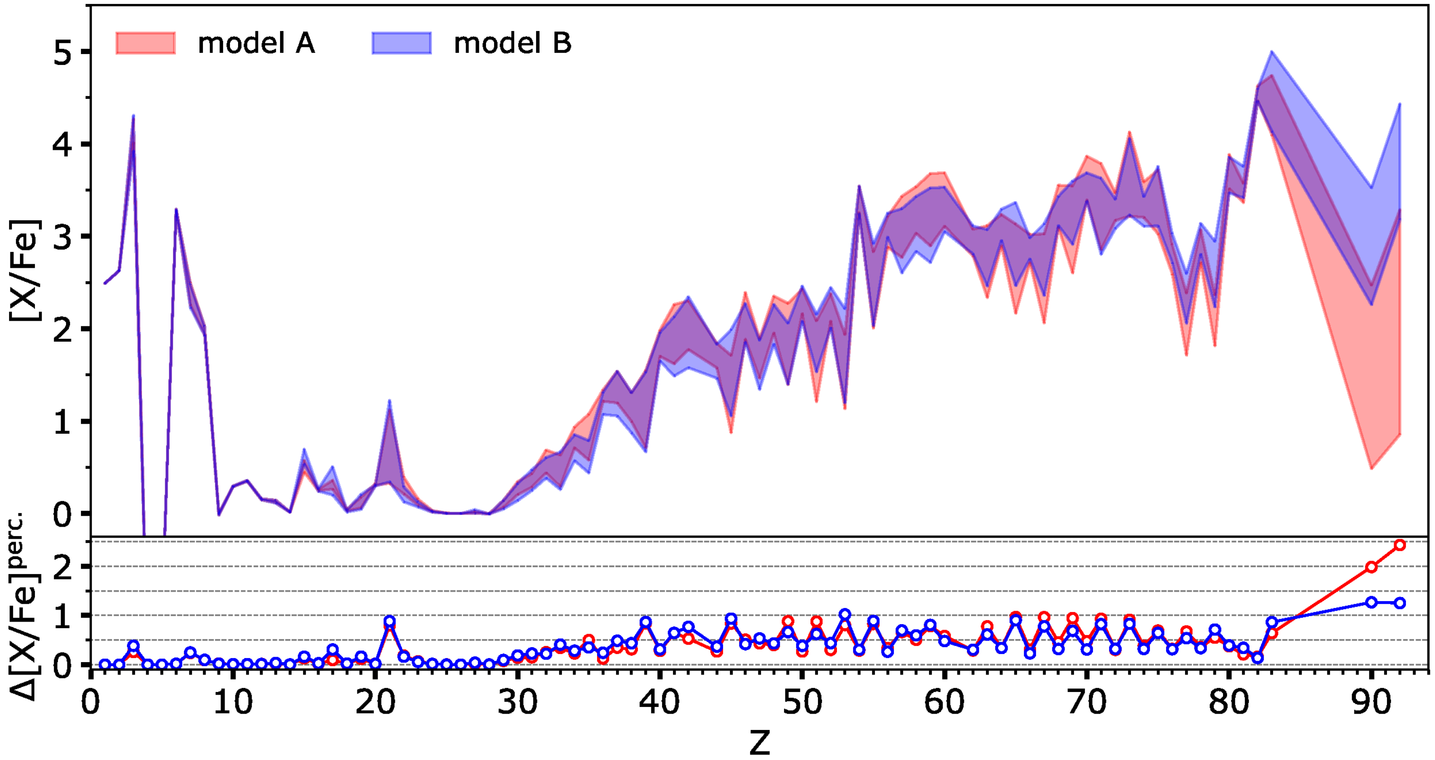

Reduction of the parameter uncertainties through

- Improved models of NLD & PSF (to reduce parameter dispersion)
- More experimental constraints

Impact of on the i-process nucleosynthesis in low-*M* low-*Z* AGB stars

Uncorrelated PSF & NLD parameter uncertainties

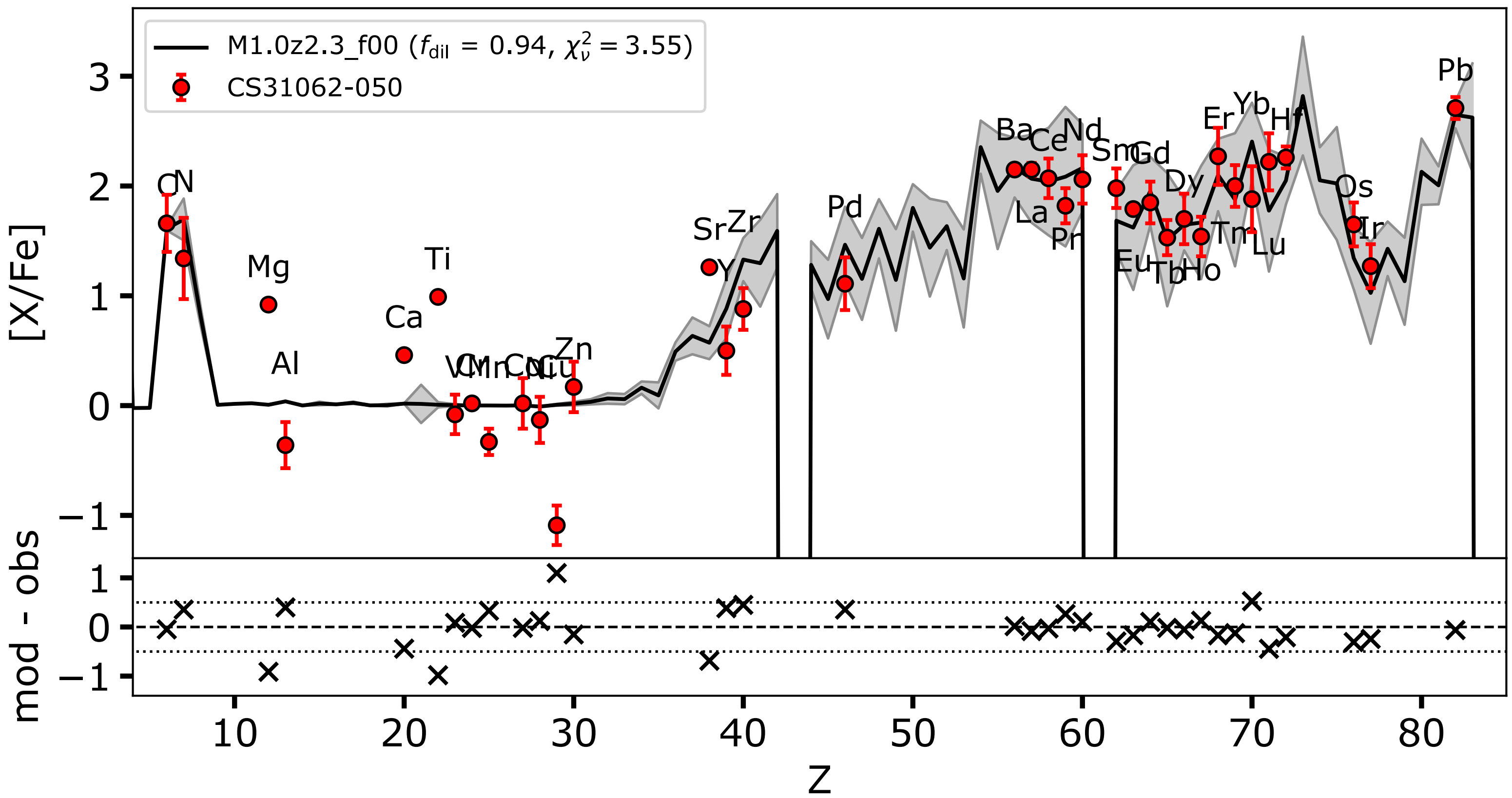

Impact of on the p-process in SN explosion of rotating massive stars

Correlated model uncertainties

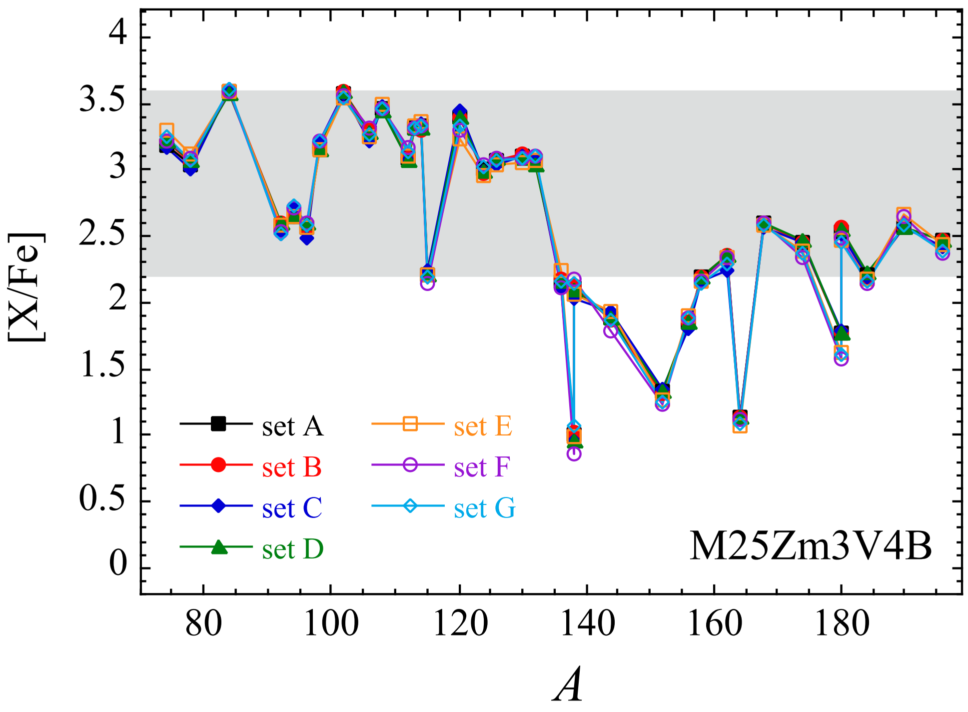

Uncorrelated parameter uncertainties

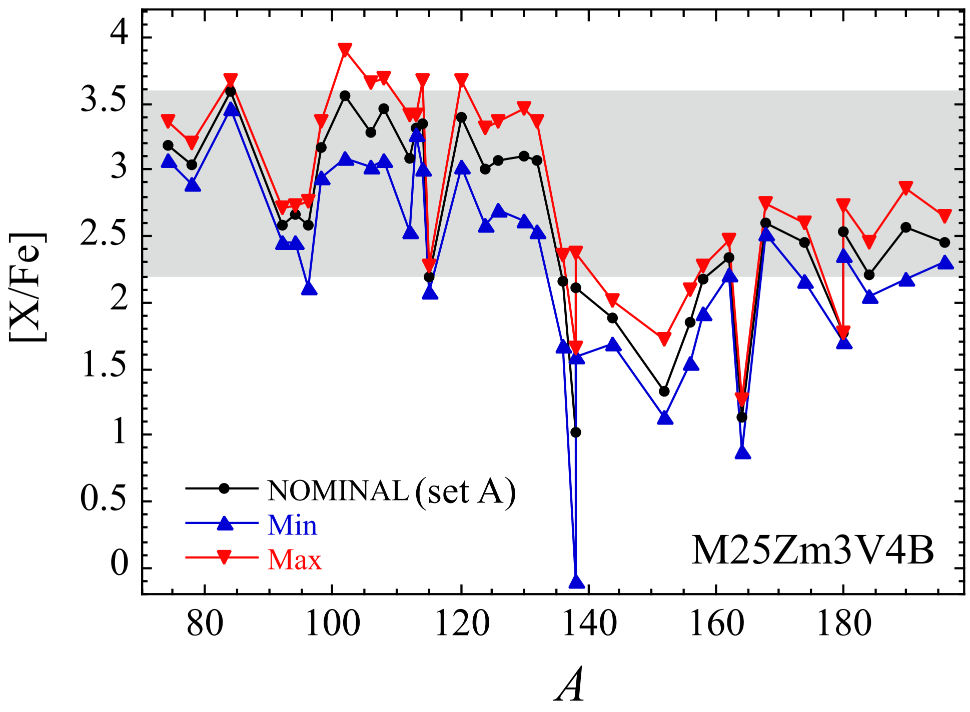

Reduction of the parameter uncertainties through

- Improved models of NLD & PSF
- More experimental constraints

Impact of PSF & NLD model uncertainties on the r-process in NSM

Correlated model uncertainties

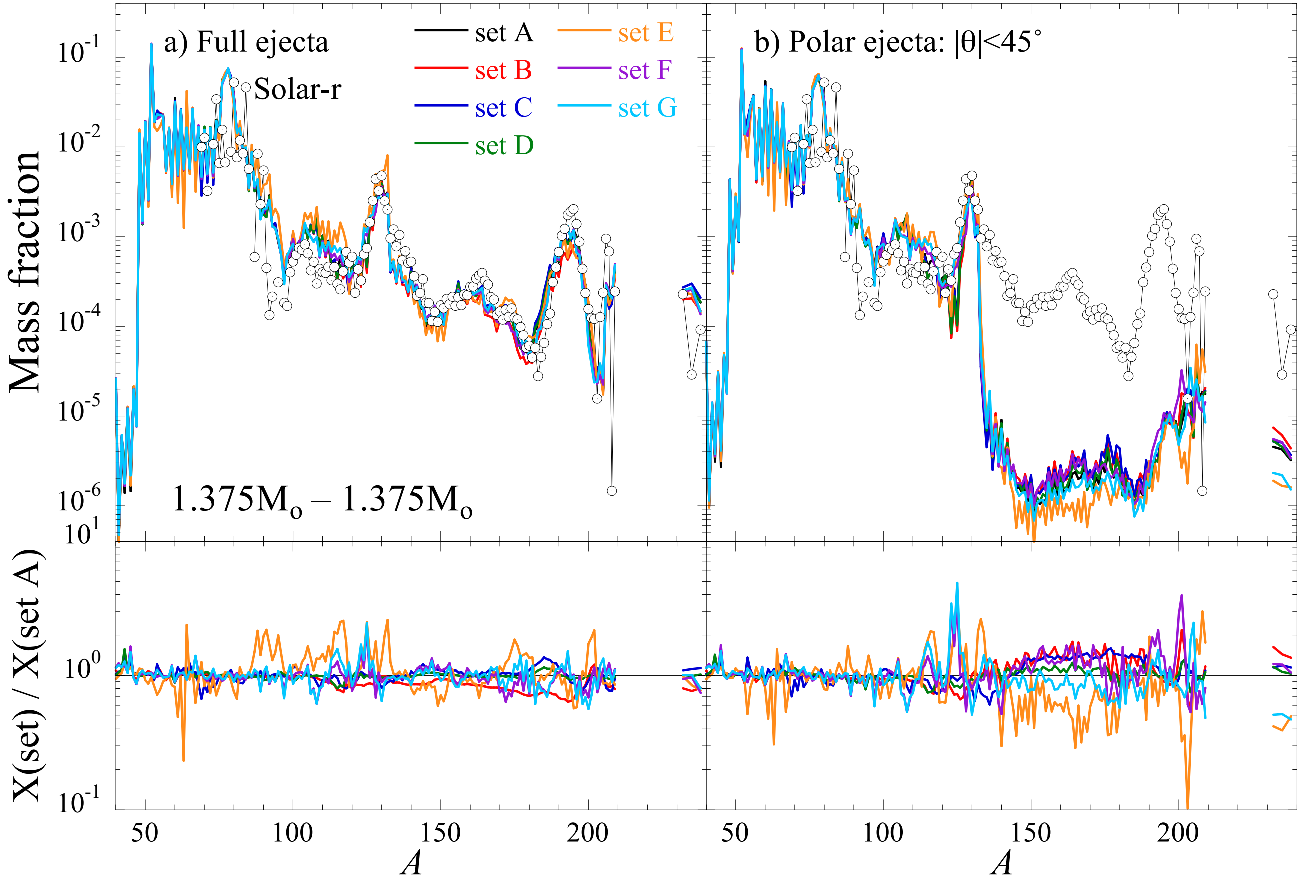

Relatively small impact on the r-process if (n,γ)-(γ,n) equilibrium achieved despite relatively different rates
(may not be the case for other progenitors)

Conclusions

PSF models have been developed and shown to globally describe experimental data and to affect radiative n-capure cross sections:

→ Low-energy *E1* QRPA strength for exotic n-rich nuclei: up to x 50

→ Non-zero limit of the *E1* strength from SM has small impact : ~20-50%

→ Spin-flip *M1* strength has small impact on (n,γ) cross section : ~10%

→ *M1* Scissors mode can impact (n,γ) cross section : up to x 2

→ *M1* upbend can affect cross sections of exotic n-rich nuclei: up to x10

Future work will require

- Understanding the discrepancies between some experimental techniques, in particular Oslo vs NRF
- Experimental constraints on the low-*E* PSF and in particular the *E1* & *M1* zero limit (upbend ?)
- Improved microscopic description of the de-excitation strength
- Large-scale calculations beyond 1p-1h QRPA (2RPA, QPM, ab-initio, ...)
- Application to odd systems

Thank you for your attention